Report No. 492
May 1954

A HYDRODYNAMIC STUDY OF THE CHINES-DRY PLANING BODY

by

John D. Pierson, Consultant
David A. Dingee
Joseph W. Neidinger

Experimental Towing Tank
Stevens Institute of Technology
Hoboken, New Jersey

EXPERIMENTAL TOWING TANK
STEVENS INSTITUTE OF TECHNOLOGY
HOBOKEN, NEW JERSEY

A HYDRODYNAMIC STUDY OF THE CHINES-DRY PLANING BODY

by

John D. Pierson, Consultant
David A. Dingee
and
Joseph W. Neidinger

PREPARED UNDER
U.S. NAVY
OFFICE OF NAVAL RESEARCH
CONTRACT NO. N6onr-24704, PROJECT NO. NR062-012
(E.T.T. PROJECT NO. CC839)

May 1954

Report No. 492

TABLE OF CONTENTS

SUMMARY

A theoretical method is developed for determining the pressure distributions and loads on prismatic Vee-shaped bodies during chines-dry planing at high speed. The method is based on the analogy which exists between the motion of the planing body through a stationary plane, oriented normal to its stagnation line, and the penetration of a two-dimensional wedge. The complete pressure distribution over an immersing wedge is available so that, on the basis of the above analogy, pressure distributions and, ultimately, total loads on the planing body are obtained.

Experiments on prismatic Vee-shaped bodies planing with chines dry were performed in order to obtain data in addition to those contained in the literature for comparison with the theory. Information on only the lift and wetted area is given.

The results of the theoretical investigation are, for the most part, presented in graphical form. These are compared with the experimental data obtained from the present reported tests and with other available data. The comparison shows that a good agreement exists between the theoretically predicted and experimentally determined pressures and loads over fairly wide ranges of planing parameters. No attempt is made to describe the pressure losses in the vicinity of the step which occur in the true three-dimensional planing case; these tend to reduce the loads as predicted by the theory.

The mathematical portions of the theory developed in this report do not lead to any closed-form expressions for the lift on a chines-dry planing body, so an empirical expression is derived from the experimental data. One of the practical uses of this empirical expression and of the theory is shown in the development of stability derivatives which are applicable to a linear porpoising stability analysis of the chines-dry planing body.

This study was carried out at the Experimental Towing Tank, Stevens Institute of Technology, under Contract No. N6onr-24704 with the Office of Naval Research.

INTRODUCTION

The present study is part of a general program of research on planing surfaces which has been undertaken by the Experimental Towing Tank of Stevens Institute of Technology under Contract No. N6onr-247, Task Order 04, with the Office of Naval Research.* The current report deals with both theoretical and experimental aspects of the pressure dis-

* Experimental Towing Tank reports and papers completed to date under this contract are listed in APPENDIX A.

tribution and load on a chines-dry, prismatic, Vee-shaped, planing body, referred to hereinafter as simply the planing body.

The problem of obtaining the pressure distribution and total load on a planing body by studying the three-dimensional flow about the body is at present too difficult to solve because of the complexities involved in establishing a mathematical model of the observed flow. Therefore, to achieve results, it has been necessary to approach the three-dimensional planing case through its two-dimensional analogue, the immersing wedge.

In general, the procedure for applying an immersing wedge analogue to the three-dimensional planing case is as follows: A plane is considered stationary in space, in which the passage of the planing body appears as an immersing wedge. From the pressure distribution over an immersing wedge that is obtained from available two-dimensional solutions, the pressure distribution and load on the planing body can be found. The availability of a good two-dimensional solution is therefore a necessary prerequisite.

It is the purpose of this study to apply, in the manner outlined above, the potential theory of the flow and pressure distribution over an immersing wedge developed in Reference 1. It is felt that the results thus obtained will be useful in determining loads and pressures for the chines-dry planing of both surface craft and seaplanes. They may also be applicable to the calculation of the pressures in the vicinity of the leading edge of the wetted area for the chines-wetted planing case.

The present work supersedes Reference 2, a previous E.T.T. report in which a theory of the planing body is derived in nearly the same way as it is presently derived, that is, by applying an immersing wedge analogue. At the time of preparation of Reference 2, the complete solution of the wedge immersion problem of Reference 1 was not available. Consequently, the authors of Reference 2 used two separate theories developed by Wagner, that of the expanding plate analogy to the immersing wedge which does not involve a spray formation, and that of a spray-root formation of a planing flat plate. Since the unified treatment of the entire wedge problem, including the formation of spray-root areas, became available in Reference 1, it appeared desirable, in the present study, to complete the three-dimensional planing body theory on this basis. Another distinction between this work and Reference 2 is that, here, the immersing wedge analogue is applied in a plane normal to the stagnation line of the planing body rather than in a plane normal to the keel.

Since published data for chines-dry planing are limited to a set of points obtained by Shoemaker (Reference 3), it was considered necessary to carry out an experimental investigation to corroborate the theoretical results of this study. To this end, tests were performed on available 9-in.-beam, Vee-shaped bodies having deadrise angles of 10°, 20°, and 30°. The test trim range was from 2° to 12°, in 2° intervals; one test speed, 24.6 ft./sec., was used. The data presented are limited to the lift coefficient and wetted bottom form for all test conditions.

SYMBOLS

A_p	wetted area delineated by the keel, step, and spray-root lines of the planing body projected onto the plane of the undisturbed water surface
a, b	constant distances locating the leading edge of the wetted area relative to the center of gravity of the planing body
C_L	lift coefficient = $L/\frac{\rho}{2} V_R^2 L_k^2$, a function of the trim and deadrise angles of the planing body
C_p	distance from the longitudinal centerline plane of the planing body to the spray-root line in the step plane
C_p'	distance from the centerline of the two-dimensional wedge to the spray root
C_s	distance from the longitudinal centerline plane of the planing body to the stagnation line in the step plane
C_s'	distance from the centerline of the two-dimensional wedge to the symmetrical points of maximum pressure
dM_1, dM_2	incremental pitching moments arising from dZ_1 and dZ_2
dZ_1, dZ_2	incremental lift forces acting on the planing body
e	a function of the two-dimensional deadrise angle = C_p'/γ' (see APPENDIX C)
F_1, F_2	functions of α
J	a function of the planing body deadrise angle, taken as $(2/\pi)\tan\beta$
K	a function of the two-dimensional wedge deadrise angle = C_s'/γ', or, equivalently, C_s/γ (see APPENDICES B, C)
L, Δ	vertical force on load
L, M, N	moments about the leading edge of the wetted area as defined in the report
L'	resultant perturbed wetted keel length of the planing body
L_k	steady planing wetted keel length of the planing body
ℓ	distance measured from the leading edge of the wetted area in the direction of the stagnation line
N	force normal to the planing body
p	pressure at any point on the wetted surface of the two-dimensional immersing wedge

p, q, r	angular velocities about the x, y, and z axes, respectively
p_a	average pressure over a wetted section of the planing body
p_k	keel pressure
p_m	maximum pressure
t	time
u, v, w	velocities in the x, y, and z directions, respectively
V	resultant perturbed planing velocity
V_e	equivalent planing velocity of a body whose instantaneous resultant velocity is not parallel to the water surface
V_i	horizontal planing velocity associated with a vertical penetration velocity of the planing body
V_R	steady planing velocity of the planing body
v'	velocity of the maximum pressure point outboard along an immersing wedge
v_o	immersion velocity of the two-dimensional wedge
v_s	vertical penetration velocity of the associated two-dimensional wedge attendant with a pitching angular velocity
X, Y, Z	forces in the positive x, y, and z directions, respectively
x, y, z	coordinate axes fixed in the leading edge of the wetted area
y	distance from the longitudinal centerline plane of the planing body to the level water intersection point in the step plane
y_o'	distance from the centerline of the two-dimensional wedge to the level water intersection point
α	angle between the keel and stagnation line on the planing body
$\alpha_1, \beta_1, \gamma_1;$ $\alpha_2, \beta_2, \gamma_2$	direction cosines as defined in APPENDIX B
β	deadrise angle of the planing body
β_a	deadrise angle of the associated two-dimensional wedge
γ	angle between the keel and spray-root line on the planing body
θ	pitch angle of the planing body about the center of gravity

λ'	aspect ratio = L_k/C_p, a function of the trim and deadrise angles of the planing body
$\lambda_1, \mu_1, \nu_1;$ λ_2, μ_2, ν_2	direction cosines of the stagnation line and keel of the planing body
ν, τ, ω	angular displacements in the reference system as defined in the report
ρ	mass density of water

In addition to the above symbols, the following notation has been used in this report (predominantly in the section on stability):

$\dot{G}$	the dot indicates time differentiation of the variable G, G arbitrary
$\bar{G}$	the bar indicates a perturbation quantity (i.e., $\bar{G} = G - G_o$)
G^*	the star refers to axes fixed in space as discussed in the text
G_{CG}	the subscript CG denotes that the quantity G is either a distance or a velocity of the center of gravity of the planing body relative to a space-fixed set of axes
G_o	the subscript o indicates the equilibrium value of the quantity G
$G_{\tau, u, w, \ldots, \text{etc.}}$	the subscripts $\tau, u, w, \ldots,$ etc. denote partial differentiation of the quantity G with respect to these parameters

THEORETICAL ANALYSIS

GENERAL CONSIDERATIONS

In order to determine theoretically the approximate pressure distribution and total load on a high-speed planing body, use will be made of the following general (and usual) assumptions:

(1) The fluid is ideal -- inviscid and incompressible.

(2) The forces due to gravity may be neglected in comparison with the relatively large dynamic forces.

In order to avoid the mathematical difficulties of a complete three-dimensional analysis of the flow and pressures in the vicinity of the planing body, it is convenient to treat this three-dimensional case in terms of its two-dimensional analogue, the immersing wedge. Thus, the passage of the planing body through a stationary plane is taken as being equivalent to the penetration of a wedge in this plane. A basis for this analogy is apparent if it is noted that there is a marked similarity between the flow fields in the spray-root regions of both the planing body

and the immersing wedge. Additional special assumptions, resulting from observation and experimentation, are required to complete this analogy. These are:

(3) A stagnation line exists on the planing body. This line, which is defined as the locus of points of maximum pressure on the wetted bottom area of the planing body, is the physical dividing line aft of which the fluid proceeds essentially in the after direction and forward of which the fluid is deflected laterally as spray.

(4) The fluid velocity along the stagnation line is constant; it is equal to the component of the resultant planing velocity in the direction of the stagnation line.

The existence of the stagnation line is well established. The constancy of velocity or pressure along it can be verified to a somewhat lesser extent if a study is made of available pressure data.

The next step in the analogy is to select the orientation of the above-mentioned stationary plane in space in which the planing body will appear as an immersing wedge. Finally, a two-dimensional theory for the pressures on an immersing wedge has to be selected in order to obtain pressure distributions over the bottom of the planing body.

PREVIOUS ANALYSIS

An earlier theory for the pressure distribution and load on a planing body, derived by the method described above and based on the assumptions listed on page 5 and above, is presented in Reference 2. Since the subject matter of Reference 2 is so closely related to the present investigation and since some use will be made of results obtained therein, it is considered important to outline briefly the techniques and limitations of this earlier analysis of the planing problem.

In Reference 2, the stationary plane of wedge immersion was taken normal to the keel of the planing body. The general pressure distribution in this plane was then obtained by using two theories, both two-dimensional. The first of these, based on the analogy in Reference 4 of the expanding plate to the immersing wedge, yielded the pressure distribution from the keel of the immersing wedge to the maximum pressure point. It failed, however, to predict pressures beyond this point on the wedge because the expanding plate analogy fails to predict accurately the free fluid surface deformation in the spray-root region. The second theory, the spray-root analysis of Reference 5, was used to obtain the remaining pressure distribution from the maximum pressure point outboard along the wetted portion of the wedge.

The maximum pressure on the stagnation line of the planing body was also evaluated in Reference 2, independently of any immersing wedge analogue. This evaluation was made possible by assumption (4) listed on

page 6, which gives information on the magnitude and direction of the velocity along the stagnation line. The maximum pressure was found by applying Bernoulli's equation between points infinitely far from the surface and on the stagnation line. With the validity of the maximum pressure as obtained from this velocity resolution technique accepted, this pressure was then expressed in Reference 2 in a form mathematically analogous to the expressions for the maximum pressure as derived from the expanding plate analogy to the immersing wedge. This expression gave rise to the concept of an "effective deadrise," defined to be the deadrise angle of that wedge immersing with velocity $V_R \sin\tau$ (the component of the planing velocity normal to the keel) whose maximum pressure was the same as that given by the velocity resolution technique, and whose mathematical formalism agreed with that of the expanding plate analogy to the immersing wedge. Pressure distributions in planes normal to the keel were then assumed to be given by the combined theories of the spray-root analysis and the immersing-wedge analysis. In the resulting expressions, the wedge deadrise angle was replaced by the effective deadrise angle. Total loads were obtained by integrating these pressure distributions over the wetted area.

The good agreement between the theoretically and experimentally determined wetted shape of the planing body and the load coefficient shown on Figures 28 and 30, respectively, of Reference 2 tends to justify the application of a two-dimensional approach to the three-dimensional planing case. However, it must be remembered that the usefulness of the analysis of Reference 2 is dependent upon the introduction of a fictitious deadrise angle of the immersing wedge; also, the theory of the immersing wedge used therein has been superseded by the theory of Reference 1. These facts suggest that an improvement to the analysis of Reference 2 might be obtained.

THE PRESENT ANALYSIS

In the present analysis, a theory is derived for the pressure distribution and load on a planing body, using the methods and assumptions listed on pages 5 and 6. The analysis differs from the analysis of Reference 2 in at least two respects: (1) the stationary plane of the two-dimensional immersing wedge analogy is not selected normal to the keel, and (2) the theory of Reference 1 is used to obtain pressure distributions in the stationary plane. A discussion of these two salient differences and a discussion of the assumed flow phenomena in the stationary plane are given below. The application of this theory in obtaining local pressures, total loads, and stability derivatives of use in a linear stability analysis is reserved for later sections.

SELECTION OF THE STATIONARY PLANE

In a two-dimensional solution of wedge penetration, the plane of immersion is perpendicular to both the keel of the wedge and the maximum pressure line. Since the maximum pressure line and keel of the three-

dimensional planing body are not parallel, it is impossible to select a stationary plane in which the passage of the planing body will appear in all respects as a penetrating two-dimensional wedge. However, since the major portion of the load comes from the immediate neighborhood of the maximum pressure line for wedge deadrise angles up to about 40°, it may be supposed that any analogy which treats wedge penetration should preferably treat it in planes normal to this maximum pressure line. Thus, inasmuch as the stagnation line of the planing body is assumed to correspond to the maximum pressure line of the immersing wedge in the present analysis, the planes of wedge immersion are taken normal to this stagnation line, which is defined by the planing geometry developed in Reference 2. A preliminary attempt to analyze the pressures and loads on a planing body by treating it as a series of wedges immersing in planes normal to the stagnation line was made in Reference 4; the solution was by no means completed, however, and the pressures over the wedge in this plane were obtained in the same manner as in Reference 2.

THE TWO-DIMENSIONAL THEORY OF THE PENETRATING WEDGE

The two-dimensional theory of the immersing wedge which is used in this report was originally proposed by Wagner (Reference 6), and then expanded and carried out in detail by Pierson in Reference 1. This theory develops, by means of an iterative process, the shape of the perturbed free fluid surface accompanying a wedge penetration, which in turn leads to the time-dependent potential in the two symmetrical spray-root regions on the two sides of the wedge, and finally to the complete velocity and pressure distribution over the wedge. This theory of the immersing wedge has the obvious advantage over the combination of two two-dimensional theories used in Reference 2 in that it yields pressure distributions over the wedge which are correct (limited only by the accuracy of iteration process), within the limits of potential theory. Unfortunately, this wedge theory is carried out for only a limited number of wedge deadrise angles, namely, 20°, 30°, 40°, and 50°, and each of these is presented in graphical form. This latter fact leads to the presentation of results of the present three-dimensional solution in graphical form rather than in closed form.

FLOW PHENOMENA IN THE STATIONARY PLANE

The reader is referred to Figures 1 and 2 (pages 40 and 41) for the following discussions. Figure 1 is a pictorial representation of the planing body and embodies most of the essential features and notation referred to herein. Figure 2 shows the associated immersing wedge in its relation to the three-dimensional planing body as the latter passes through the stationary plane, and the notation in this plane. It is pointed out that an analogy exists between the flow about only one side of the planing body, in the stationary plane, and the flow about only one side of the immersing wedge.

In Figure 1, the line of intersection between the stationary plane perpendicular to the stagnation line and one side of the planing body is

denoted by K_2S, and the line of intersection between the stationary plane and the water surface is denoted by K_2W. The angle between these two lines is called the associated deadrise angle, β_a (see Figures 1 and 2). This angle, β_a, is then the geometric deadrise angle of the immersing wedge associated with the passage of the planing body as viewed in the stationary plane as defined. The associated deadrise angles as functions of the planing body trim (τ) and deadrise (β) angles have been computed by a method set forth in APPENDIX B; a graph of β_a vs. β for various τ appears in Figure 3.

In addition to defining the geometry of the associated wedge in terms of the geometry of the planing body, it remains to define the immersion velocity of this wedge in terms of the steady planing velocity of the planing body. The physical condition which permits this evaluation is that, to an observer situated in the stationary plane, the passage of the planing body stagnation line appears as the traveling maximum pressure point of the associated immersing wedge. It is then clear that the velocity of the maximum pressure point out along the wedge is equal to the corresponding velocity of the stagnation line in this plane, normal to itself along the planing body. This condition becomes more important if it is realized that the penetration velocity, and hence the pressure distribution over the immersing wedge, may be defined in terms of the velocity of the maximum pressure point outboard along the wedge. Thus, from the geometry of the planing body, the velocity of the stagnation line normal to itself in the plane of the body may be determined; this in turn fixes, within the limits of the present study, the pressure distribution in normal planes and ultimately the total load. The details of the computation which gives the penetration velocity, v_o, of the associated wedge in terms of the planing velocity, V_R, and geometric quantities are contained in APPENDIX C, with the resultant expression

$$v_o = \frac{\sin\beta_a \sin\alpha}{K \cos\tau} V_R \quad , \tag{1}$$

where α is a function of the planing body trim and deadrise angles, and K is a function of the associated deadrise angle. Both α and K as used are defined in APPENDIX C.

Finally, having obtained the associated deadrise, β_a, and the penetration velocity, v_o, the pressure distribution in normal planes is taken as the pressure distribution given in Reference 1 for the immersing wedge of deadrise β_a. Since Reference 1 provides pressure distributions for deadrise angles of 20°, 30°, 40°, and 50° only, the results must be interpolated or extrapolated to obtain pressure distributions for an arbitrary wedge deadrise angle. The total load acting on the planing body is then found by integrating these pressure distributions over the wetted area, but more will be said of this later.

SUMMARY

In the present theory, (1) use is made of the four general and specific assumptions listed on pages 5 and 6; (2) the stationary plane is

selected normal to the stagnation line of the planing body; (3) the planing body geometry in this plane defines β_a, the deadrise of the two-dimensional wedge associated with the passage of the planing body through this plane; (4) the velocity of the stagnation line of the planing body in this plane is used to determine the corresponding penetration velocity of the associated two-dimensional wedge; and, finally, (5) use is made of a single two-dimensional theory (Reference 1) of the immersing wedge to obtain pressure distributions in the normal planes and hence the total loads on the planing body.

EXPERIMENTAL STUDY

Relatively little experimental data pertaining to the chines-dry planing of prismatic Vee-shaped surfaces are available. In fact, the only extensive chines-dry planing data published prior to the present investigation were obtained by Shoemaker (Reference 3). Some work on impact prior to chine immersion may be treated as chines-dry planing if the appropriate velocities are used, but even so, relatively little applicable data of this type are on hand (see, for instance, References 7 and 8). In view of these facts, it was felt necessary to obtain additional chines-dry planing data to corroborate the theory of this report.

MODELS

Three Vee-shaped prismatic models having deadrise angles of 10°, 20°, and 30° were selected from among those used in previous E.T.T. tests. Each of the models has a beam of 9 in., a length of 54 in. from transom to bow, and an over-all height of 9 in. Further details concerning the construction and cross-sectional shapes are contained in Reference 9.

TOWING EQUIPMENT

The tests were performed in Tank No. 3 of the Experimental Towing Tank. The carriage which was used allowed the models freedom in heave only. Resistance and pitching moment were obtained from suitable electronic balances. Wetted bottom configurations were determined from underwater photographs, two of which are shown in Figure 4. The photograph in Figure 5 shows one of the models completely equipped for testing. Reference 9 gives further information regarding the towing equipment and associated test techniques.

In an attempt to minimize errors in load or drag readings due to aerodynamic forces, a large aluminum air screen was towed directly ahead of the model, as shown in Figure 5.

Although usually employed in similar tests at the E.T.T., no turbulence-inducing strut was used in the current tests. It was felt that, in

view of the small wetted areas to be encountered, too large a disturbance of the flow pattern might result from the use of such a turbulence-stimulating device.

TEST CONDITIONS AND PROCEDURE

Each of the three models was run in a straight line on a smooth water surface at a constant speed of 24.6 ft./sec., at fixed trim with no yaw. The models were free to heave and hence assumed a vertical position at which the load on the model was supported by the dynamic reaction of the water. For each of the test trim angles τ = 2°, 4°, 6°, 8°, 10°, and 12°, the load was adjusted so that the stagnation line emerged from the step plane no closer than 1/8 beam from the chine. In most cases, the load was also varied at a given trim in order to serve as a check on the computed load coefficient, C_L.

The following general test procedure was used for a typical planing run: The model was set at the proper trim angle and, as the case demanded, loaded or unloaded to the desired weight. The carriage was then accelerated to running speed by automatic control. As the model passed the underwater camera which was set up to take photographs of the bottom planing area, an electric eye arrangement triggered the camera. During this time, electronic readings of the drag and pitching moment were taken. A visual observation of the towed model indicated at which position the stagnation line was emerging at the step and thus suggested what loading to use in the check runs. The model was then returned to its starting position and the process was repeated for different combinations of load and trim. The detailed planing test conditions for each model, together with the test results, are given in Table I (pages 38 and 39).

Despite the precautions taken to eliminate aerodynamic forces, it was believed that some would remain in the presence of the air screen. These were estimated by towing the model just off the water surface behind the air screen, repeating the conditions of speed and trim which had been investigated with the model in the water. These aerodynamic forces and moments were subtracted from the original test quantities to arrive at the hydrodynamic forces and moments.

TEST RESULTS

It was hoped, at the outset of the current study, that the test results might be presented in the form of lift coefficients and dimensionless centers of pressure. However, the experimental technique that was used led to difficulty in the determination of the centers of pressure. The computations for the center of pressure depended, of course, on both the drag and pitching moment measurements as well as on the lift. This dependence unfortunately was in the form of small differences of large quantities. Small errors in the large quantities such as pitching moment or drag therefore led to sizable errors in the determination of the cen-

ters of pressure. For this reason, the presentation of test results is limited to the lift coefficient; this is tabulated with the corresponding test conditions in Table I and presented graphically in Figure 6. A small amount of E.T.T. unpublished data for the case of the 40° deadrise surface and all of the data from Shoemaker's investigation in Reference 3 are also shown in this Figure. The scatter of the Shoemaker data is indicated by the boxes surrounding the mean values of C_L.

On the whole, there is agreement between Shoemaker's data and E.T.T. data, but there seems to be some tendency for the E.T.T. data to fall higher than Shoemaker's. This difference may be attributed to a variance in the methods used to determine wetted length in each of the investigations. Shoemaker determined this length from over-water observations, and E.T.T., from underwater photographs. The tendency of the water to surge forward in a "roll up" along the model bottom could more easily be taken as a longer wetted length in over-water observations than would appear in underwater photographs, leading to lower values of the lift coefficient C_L as defined in this report.

RESULTS AND DISCUSSION

COMPARISON OF THEORY WITH EXPERIMENT

THE MAXIMUM PRESSURE

The prediction of the maximum pressure, denoted as p_m, is an important aspect of a theoretical investigation of the planing body since it is this pressure that gives rise to the maximum local load. It is evident from its definition that p_m will occur on the stagnation line of the planing body; hence, in the present analysis, it will be taken as being equal to the maximum pressure of the associated immersing wedge.

The maximum pressure on the associated immersing wedge can be found in terms of the planing body geometry and the planing velocity. The following procedure will illustrate the use of the various graphs of this report in finding this maximum pressure:

(1) Given the planing geometry (i.e., trim and deadrise angles of the planing body), the associated wedge deadrise angle, β_a, can be obtained from Figure 3, which results from the computations outlined in APPENDIX B.

(2) Having obtained β_a, Figure 7 is then referred to for the corresponding value of the dimensionless maximum pressure based on penetration velocity, $p_m/\frac{\rho}{2} v_o^2$. Two curves appear on Figure 7, one solid and one dashed. The dashed one results from the expanding-plate analogy solution of the immersing wedge (Reference 4) mentioned previously, which is a closed form expression for $p_m/\frac{\rho}{2} v_o^2$ vs. wedge deadrise angle. The solid curve is faired through the values of $p_m/\frac{\rho}{2} v_o^2$ taken from Reference 1; it was ex-

trapolated to $\beta_a = 10^o$ by a qualitative and quantitative comparison with the dashed curve.

(3) Finally, the relationship of equation (1), shown graphically in Figure 8, allows for the evaluation of the dimensionless maximum pressure based on planing velocity, $p_m/\frac{\rho}{2} V_R^2$.

A resultant graph of $p_m/\frac{\rho}{2} V_R^2$ vs. τ, obtained by following the above procedure, is shown in Figure 9 for four planing bodies having deadrise angles of 10^o, 20^o, 30^o, and 40^o.

Another theoretical method of determining $p_m/\frac{\rho}{2} V_R^2$ for any planing condition is discussed in the section of this report entitled PREVIOUS ANALYSIS. In this method, the maximum pressure results from an application of Bernoulli's equation between points at infinity and on the stagnation line of the planing body (Reference 2). The resultant expression so derived is

$$\frac{p_m}{\frac{\rho}{2} V_R^2} = \sin^2\tau \left[\frac{(K - \sin^2\beta)^2}{\sin^2\beta + K^2\tan^2\tau} + \cos^2\beta \right] \quad * \quad , \qquad (2)$$

where all the symbols are as defined herein, K being defined in APPENDIX B as a function of the planing body deadrise angle, β.

The only experimental data available on the maximum pressure of a planing body are contained in References 7 and 8. These data are actually the result of landing tests performed on bodies whose instantaneous resultant velocity had components parallel and normal to the water surface. The equivalent "planing" velocity for the case of landing has been defined as the resultant horizontal velocity of the stagnation line. Thus, if $\dot{x}$ and $\dot{z}$ are used to denote the components of the instantaneous resultant velocity of the body in directions parallel and normal to the undisturbed water surface, respectively, the equivalent planing velocity, V_e, is given by

$$V_e = \dot{x} + \frac{\dot{z}}{\tan\tau} \quad . \qquad (3)$$

The test results of References 7 and 8 have been summarized by the empirical relation

$$\frac{p_m}{\frac{\rho}{2} V_e^2} = \sin^2\tau \left(\frac{1}{\sin^2\tau + J^2\cos^2\tau} \right) \quad , \qquad (4)$$

where the quantity designated J is a function of the deadrise angle. Only two values of J have been determined experimentally -- one each for body deadrise angles of $22\frac{1}{2}^o$ and 30^o; however, in Reference 7, it is pointed out that the asymptotic behavior of J as a function of β, for small β, is

---

* Equation (22) of Reference 2.

$$J = \frac{2}{\pi} \tan\beta \quad . \tag{5}$$

For the purpose of comparing the maximum pressure coefficient given by equation (2) with that given by equation (4) and the one developed in the present report, it was found convenient to use this definition for J throughout the range of β considered. Only slight discrepancies exist between this definition and the experimentally determined values of J, as can be seen on Figure 10.

For each landing condition of the bodies tested and reported in References 7 and 8, the model penetrated the water to various depths. The fact that equation (4) above is independent of depth is an experimental indication that no significant variation in peak pressure occurs when the body passes from the chines-dry to the chines-wetted condition. Therefore, it may well be assumed that the pressure distribution in the immediate vicinity of the stagnation line as theoretically developed in this report for the chines-dry planing case is also applicable to this region when the chines are wetted.

Figure 9 shows a comparison of the maximum pressure coefficients given by equations (2) and (4), and the theory developed in the present report, throughout a practical range of trim and deadrise angles. In general, the agreement among them is good. However, the values of the maximum pressure coefficient given by the three methods tend to diverge at high trim angles. This is to be expected since different limiting values of the maximum pressure coefficient are predicted by the three methods as the trim angle of 90° is approached. Since the change in the maximum pressure coefficient with trim angle is not rapid for large trims ($30^\circ < \tau < 90^\circ$), the limiting value at 90° trim will affect the values at other high trim angles. The empirical equation (4) predicts a maximum pressure coefficient of unity at 90° trim angle; equation (2) predicts that this coefficient will approach $\cos^2\beta$ at this trim angle; and the present theory is forced to leave the value of this coefficient undefined at this limiting condition inasmuch as values of β_a approach 90° with the trim angle and no asymptotic theoretical values of the maximum pressure coefficient for high deadrises are available.

THE LIFT COEFFICIENT

The lift, L, in the upward direction perpendicular to the undisturbed water surface is given by the product of the average pressure over the wetted surface of the body and the area of this wetted surface projected onto the undisturbed water plane. Thus, before a theoretical derivation of the lift coefficient can be completed, the magnitudes of the average pressure and the projected wetted area must be determined.

In order to determine the average pressure on the surface of the planing body, it is first necessary to establish the correspondence of the two-dimensional pressure distribution over the associated immersing wedges with the pressure distribution over the entire wetted portion of

the planing body. To this end, the reader is referred to Figure 11, a plan view of the planing body. Shown on this Figure are typical sections, A-A and B-B, taken normal to the stagnation line of the planing body, in which the pressure distribution is assumed to be the same as that on one side of an immersing wedge. In a section such as B-B, which does not intersect the keel of the planing body, the step of the planing body is taken to correspond to the keel of the immersing wedge. This assumption is convenient in practice since it insures that, once the average pressure in any section normal to the keel has been determined, it will be constant for all such sections, and that (providing $\beta_a < 40^\circ$) the pressure distribution over the step of the planing body will be constant and a minimum (see section C-C of Figure 11), which approaches the true case. It is understood, of course, that, in reality, the pressure quickly drops to zero at the step. This drop, however, affects only a small part of the complete pressure distribution and is neglected in the present work.

Having set up a correspondence of the two-dimensional pressure distribution of the immersing wedge with the pressure distribution over the planing body, it now remains to evaluate the average pressure from these pressure distributions. To do this, the pressure distribution curves for the immersing wedge which are reproduced from Reference 1 in Figure 12 for various deadrise angles must be integrated over the wetted width. It will be noted from this Figure that these curves extend out to values of y', the distance from the wedge centerline, greater than C_p', the distance from this centerline to the spray root (see Figure 2). However, in view of the fact that the theoretical expression for the distance C_p' is so simple and relatively well established, it was decided to define the weighted average pressure coefficient as

$$\frac{p_a}{\frac{\rho}{2} v_o^2} = \frac{1}{C_p'} \int_0^{1.2\, C_p'} \frac{p}{\frac{\rho}{2} v_o^2}\, dy' \quad . \tag{6}$$

In order to define the lift, this weighted average pressure is then applied to the reduced wetted area delineated by the keel and spray-root lines of the planing body. In this manner, the total force is included, but it is assumed that it acts over a slightly smaller wetted portion of the planing body than exists in reality. A curve of $p_a/\frac{\rho}{2} v_o^2$ vs. β_a fitted through four points as computed by the above procedure is presented in Figure 13 (solid line). This curve is extended to a deadrise angle of 0° by comparing the average pressures obtained above with those obtained by the combined two-dimensional theories used in Reference 2 (the dashed curve of Figure 13). This method is analogous to the procedure used to extend the maximum pressure coefficient curve of Figure 7, as discussed on page 12.

An expression for the wetted area, A_p, delineated by the keel, step, and spray-root lines of the planing body projected onto the plane of the undisturbed water surface is found with reference to Figure 1 to be

$$A_p = L_k C_p \cos\tau \quad , \tag{7}$$

where L_k represents the wetted keel length $\overline{OK}$ of Figure 1 and C_p is the wetted half beam. But from equation (15) of Reference 2,

$$C_p = \frac{\pi}{2} L_k \frac{\tan\tau}{\tan\beta} \quad ; \tag{8}$$

therefore,

$$A_p = \frac{\pi}{2} L_k^2 \frac{\sin\tau}{\tan\beta} \quad . \tag{9}$$

A comparison graph of the values of A_p/L_k^2 determined from the underwater photographs of the present experiments and those which result from equation (9) above appears on Figure 14. The differences between these values may be attributed directly to the differences between the observed and predicted values of the wetted semi-width, C_p, which result from the rapid loss of pressure in the region of the step and subsequent bending toward the keel of the stagnation line in this region (see, for example, Figure 4, where the represented test conditions approach extreme values of the planing parameters). Thus, by substituting the observed values of C_p into equation (7), a considerably smaller value for A_p/L_k^2 results than if use were made of the values of C_p predicted on the basis of the assumption that there is no curvature of the stagnation line. It is pointed out, however, that the true value of the wetted area defined by the observed stagnation lines and step differs from the theoretical value in the vicinity of the step only. This is a consequence of the fact that the observed stagnation line is essentially straight and, except in the step region, is in the predicted location. This small difference will be neglected in the succeeding development.

Having determined the average pressure and the projected wetted area, expressions for the lift and finally the theoretical lift coefficient can now be given. The lift is defined as

$$L = p_a A_p \quad , \tag{10}$$

and the lift coefficient based on planing velocity and wetted keel length, as in Reference 2, is

$$C_L = \frac{L}{\frac{\rho}{2} V_R^2 L_k^2} \quad . \tag{11}$$

Substituting the right-hand side of equation (9) into equation (10) and the result into equation (11) gives

$$C_L = \frac{p_a}{\frac{\rho}{2} V_R^2} \frac{\pi}{2} \frac{\sin\tau}{\tan\beta} \quad . \tag{12}$$

Since the associated wedge penetration velocity, v_o, is related to the planing velocity, V_R, by equation (1), then equation (12) can also be written as

$$C_L = \frac{p_a}{\frac{\rho}{2} v_o^2} \left(\frac{\pi}{2} \frac{\sin\tau}{\tan\beta}\right)\left(\frac{\sin\beta_a \sin\alpha}{K \cos\tau}\right)^2 . \qquad (13)$$

The quantity $p_a/\frac{\rho}{2} v_o^2$, plotted vs. wedge deadrise angle, appears on Figure 13; values of $(\pi/2)(\sin\tau/\tan\beta)$ are given on Figure 15; and values of $\sin\beta_a \sin\alpha/K \cos\tau$, the velocity ratio, can be found on Figure 8.

The theoretical values which result from equation (13) appear on Figure 6 for comparison with experimental data. The theory predicts well the type of variation of C_L with trim and deadrise angles but there is a tendency for the magnitudes of C_L predicted by the theory to be slightly greater than those measured. This is, of course, not surprising inasmuch as the theory does not take into account the edge pressure losses existing on the true planing body in the vicinity of the step.

THE LIFT COEFFICIENT IN TERMS OF ASPECT RATIO

It has been pointed out in the development of the theoretical lift coefficient that the results can be presented in graphical form only -- a consequence of using the theory of the immersing wedge of Reference 1. For certain applications of the theory of lift on the planing body, it is convenient to have on hand a closed analytic expression for the lift coefficient. The desirability of such an expression has prompted the development of the following empirical expression for C_L as a function of the planing geometry.

A significant single quantity defining the planing geometry is the wetted length-beam ratio, λ', defined to be the ratio of the wetted keel length, L_k, to the mean wetted beam, C_p, of the planing body. This concept is a familiar one to both designers and investigators and is therefore selected as a basis for the development of an empirical expression for C_L.

An expression for λ' in terms of the planing body trim and deadrise angles follows from its definition and from equation (8) to be

$$\lambda' = \frac{2}{\pi} \frac{\tan\beta}{\tan\tau} . \qquad (14)$$

It was found that, by plotting C_L vs. $\lambda' \cos^2\beta$, the theoretical and experimental values of C_L for the various deadrise and trim angle combinations considered on Figure 6 of this report could be adequately collapsed onto single curves, one theoretical and one experimental. Figure 16 shows the results of such a plot. Only the mean line is shown through the relatively small scatter of points obtained by plotting the theoretical

values. An empirical equation which represents the experimental relationship between C_L and $\lambda' \cos^2\beta$ was obtained by fitting a straight line to the experimental data points on Figure 16. This equation,

$$C_L = \frac{0.151}{(\lambda' \cos^2\beta)^{2.7}} \quad , \tag{15}$$

represents the data with sufficient accuracy in the range of C_L from 0.0006 to 0.1. No experimental data which result in C_L values less than 0.0006 are available, but it is anticipated that the empirical expression will adequately represent these high deadrise, low trim angle planing cases. For C_L greater than 0.1, the empirical curve does not agree with the experimental results; however, these C_L values correspond to the low deadrise, high trim angle planing cases and are not usually of practical interest. The planing phenomena associated with C_L greater than 0.1 are those which have been noted before to cause difficulty of analysis because of the high pressure gradient in the vicinity of the step, and the associated reduced wetted area. Some use of the above empirical relation will be made in the succeeding section on the stability derivatives.

THE STABILITY DERIVATIVES

There is, in the literature, a relative lack of analytical expressions for any of the stability derivatives which may arise in a stability analysis of the porpoising of a chines-dry planing body. A logical application of the theory derived in this report to a practical planing problem would therefore be in the development of analytical expressions for these derivatives, as shown below. Only the hydrodynamic derivatives resulting from the lift force will be discussed. No consideration will be given to the derivatives arising from either aerodynamic forces or drag forces nor to the questions connected with the solution of the equations. The derivatives to be developed will have immediate application to any linear stability analysis of the chines-dry planing body which may subsequently be made.

In the standard linear stability analysis, such as the one presented in Reference 10, axes are fixed in space with the origin located instantaneously at the center of gravity of the planing craft. Two coupled equations of motion are written which express the equilibrium of forces in translational and in rotational acceleration. All terms are usually referred to the translation of the C.G. and to the rotation of the body about the C.G. The evaluation of the necessary stability derivatives in such a system is somewhat complicated by the fact that a simple motion may have several effects (i.e., a rotary pitching motion about the C.G. results in both a change of wetted length and a change in the angle of the keel relative to the undisturbed water surface).

The reference axes chosen for the present application of the theory are fixed in the body at the intersection point of the keel with the undisturbed water surface, at the trim and heave of equilibrium (see Figure

17). With this axis system, the stability derivatives take on a particularly simple form, thereby eliminating the possibility of overshadowing the underlying principles by the mass of algebra entering with the interaction effects referred to above.

Figure 17 shows the space-fixed (x^*, z^*) axes used in a standard porpoising stability analysis and the body-fixed (x, z) axes used in the present analysis. The planing body is shown in its equilibrium state and in a perturbed state. APPENDIX D contains the necessary transformation equations which give the applicable stability derivatives in the (x^*, z^*) system in terms of those in the (x, z) system which are derived below.

The general reference system for the current analysis is set up as follows:

Linear Disposition	x	y	z
Designation	longitudinal	lateral	normal
Positive Direction	forward	starboard	downward
Linear Velocity	u	v	w
Force	X	Y	Z
Angular Disposition	ν	τ	ω
Designation	roll	trim	yaw
Positive Direction	$y \rightarrow z$	$z \rightarrow x$	$x \rightarrow y$
Angular Velocity	p	q	r
Moment	L	M	N

Here, porpoising is regarded as a coupled motion of pitching and heaving of the planing body in the x,z-plane; hence, only the Z-force and M-moment are of interest. Also, surging motion is considered as being uncoupled and will not be introduced (justified in Reference 10). Z and M are considered to be functions of z, τ, w, and q which, subsequent to a perturbation from equilibrium, can be expressed in a linearized Taylor Series expansion as

$$Z = Z_o + Z_z\bar{z} + Z_\tau\bar{\tau} + Z_w\bar{w} + Z_q\bar{q} \tag{16}$$

$$M = M_o + M_z\bar{z} + M_\tau\bar{\tau} + M_w\bar{w} + M_q\bar{q} \quad , \tag{17}$$

where all derivatives are considered to be constant and are to be evaluated at equilibrium. The first (zero subscript) terms on the right-hand side of the above equations denote the equilibrium values of the Z-force and M-moment. The bar terms represent perturbation quantities (e.g., $\bar{\tau} = \tau - \tau_o$). The remaining terms ($Z_z$, M_w, etc.) are partial derivatives with respect to the subscript quantities. This subscript notation should not be confused with the usual subscripts used to designate the nature of a parameter, as for instance, L_k, C_L, C_p, etc. Linear perturbation quantities are measured relative to space-fixed axes, taken conveniently as the initial position of the present axes immediately prior to a disturbance from equilibrium. Angular perturbations are taken about the origin of the axis system. The M-moment is measured about the instantaneous position of the leading edge of the wetted area.

The above derivatives will be evaluated in terms of the equilibrium planing geometry, and the theoretical equilibrium forces derived in the present report. Again, it is to be emphasized that the practical application of these particular derivatives to a stability analysis must be carried out in an axis system which treats the motion of, and about, the C.G. of the planing body.

Z-FORCE DERIVATIVES

It will be convenient in the evaluation of all Z-force derivatives except Z_q to express the instantaneous vertical force, Z, in terms of the dimensionless lift coefficient, C_L, as

$$Z = -\frac{\rho}{2}(L')^2 V^2 C_L \quad , \tag{18}$$

which is valid for any purely translatory motion (i.e., $q = 0$), where

ρ is the mass density of water,

V is the instantaneous perturbed planing velocity (equilibrium value $= V_R$),

L' is the instantaneous perturbed wetted length (equilibrium value $= L_k$), and

C_L is the lift coefficient, constant for a given planing geometry.

The Z-force derivatives are discussed below in the order in which they appear in equation (16).

The vertical force change with change in depth, Z_z, is expressed as

$$Z_z = Z_{L'} L'_z + Z_{C_L}(C_L)_z \tag{19}$$

(subscript notation is used and all derivatives are to be evaluated at equilibrium). Equation (18) may be used to evaluate $Z_{L'}$ as

$$Z_{L'} = -\rho V_R^2 L_k C_L = \frac{2}{L_k} Z_o \quad . \tag{20}$$

Next, from Figure 17, it is clear that

$$(L' - L_o)\sin\tau = z \quad , \tag{21}$$

where L' represents the instantaneous wetted length of the body, and L_o the equilibrium value, which is equal to L_k. Hence,

$$L'_z = \frac{1}{\sin\tau_o} \quad . \tag{22}$$

In equation (13), the lift coefficient, C_L, is shown to depend only on the trim angle for a given planing body deadrise angle; therefore,

$$(C_L)_z = 0 \quad . \tag{23}$$

Substituting equations (20), (22), and (23) into equation (19) gives finally

$$Z_z = \frac{2}{L_R \sin\tau_o} Z_o \quad . \tag{24}$$

The vertical force change with change in trim angle, Z_τ, is given by

$$Z_\tau = Z_{L'} L'_\tau + Z_{C_L}(C_L)_\tau \quad . \tag{25}$$

From equation (21), the equilibrium value of L'_τ is shown to be zero. Z_{C_L} may be evaluated from equation (18) as

$$Z_{C_L} = \frac{Z_o}{C_L} \quad . \tag{26}$$

The value of $(C_L)_\tau$ is obtained from the empirical relation, equation (15), as

$$(C_L)_\tau = \frac{5.4}{\sin 2\tau_o} C_L \quad . \tag{27}$$

so that, finally, substituting equations (26) and (27) into equation (25) yields

$$Z_\tau = \frac{5.4}{\sin 2\tau_o} Z_o \quad . \tag{28}$$

The vertical force change with change in vertical velocity, Z_w, will be derived below, following a brief outline of the approach taken in its development.

The effect of vertical velocity on a planing body at a given trim angle may be treated in terms of its equivalent effect on the horizontal motion of the stagnation line or planing velocity. This has been demonstrated in the derivation of equation (4). Thus, a vertical velocity of magnitude w gives rise to an incremental planing velocity of magnitude

$$V_i = \frac{w}{\tan\tau} \quad , \tag{29}$$

yielding a resultant planing velocity

$$V = V_R + V_i = V_R + \frac{w}{\tan\tau} \quad . \tag{30}$$

Since the planing velocity or, equivalently, the velocity of the stagnation line has played such an important role in the theoretical determination of the loads and pressures on a planing body (see, for instance, APPENDIX C), it was decided to treat the change in Z-force with vertical velocity in terms of the change in Z-force with planing velocity. Thus,

$$Z_w = Z_v V_w + Z_{C_L}(C_L)_w \quad , \tag{31}$$

where $(C_L)_w$ is zero since it is evaluated at constant wetted length-beam ratio, λ', and by equation (15) is independent of w. Finally, using equation (18) for Z_v and (30) for V_w gives

$$Z_w = (-\rho V_R L_k^2 C_L)\frac{1}{\tan\tau_o} = \frac{2Z_o}{V_R \tan\tau_o} \quad . \tag{32}$$

The vertical force change with change in angular velocity, Z_q, cannot be treated in a manner analogous to that uaed for the other derivatives since the expreasion for Z (equation (18)) is no longer valid. This is a consequence of the fact that, for the caae $q \neq 0$, the instantaneous perturbed planing velocity, V, ia indirectly a function of the distance between a aection of the body and the leading edge of the wetted area. The direct dependence of Z on q is in the penetration velocity of the associated wedges in plenes normal to the stagnation line. Accordingly, for the case $q \neq 0$, the derivative with respect to q will have to be approached by a method which takes into account the variation in conditions from one such section of the body to the next. This latter method involves aetting up expressions for the contribution to the total Z-force by an arbitrary narrow slice of the planing body in a section perpendicular to the stagnation line, differentiating it with respect to q, and finally integrating over the entire wetted portion.

An incremental slice of the wetted bottom of the planing body normal to the stagnation line defines a wedge. Relationships have been established for the associated deadrise angle, β_a, and for the average pressure coefficient, $p_a/\frac{\rho}{2}v_o^2$, of this wedge. These quantities are invariant with respect to q since they are both geometrically determined and independent of velocity. Therefore, with reference to Figure 18, the following relations are established for the incremental lift forces, dZ_1 and dZ_2, contributed by the one-sided wedges in such sections:

$$dZ_1 = \frac{p_a}{\frac{\rho}{2}v_o^2}\frac{\rho}{2}v_s^2 \tan\alpha\cos\beta_a \ell\, d\ell \qquad (0 < \ell < L_k\cos\alpha) \tag{33}$$

$$dZ_2 = \frac{p_a}{\frac{\rho}{2}v_o^2}\frac{\rho}{2}v_s^2 (L_k\sec\alpha - \ell)\cot\alpha\cos\beta_a\, d\ell \qquad (L_k\cos\alpha < \ell < L_k\sec\alpha) \tag{34}$$

where

ℓ is the distance between a section of the body and the leading edge of the wetted area measured along the stagnation line, and

v_s is the resultant penetration velocity of the equilibrium maximum pressure point in this section (see following discussion).

It may be noted on Figure 18 that q has a varying effect on the wedge penetration velocity in a section normal to the stagnation line. Thus, the keel of the wedge, being at a greater distance from the axis of q, has a greater induced penetration velocity than other points on the wedge. It is arbitrarily assumed that this variable penetration velocity along the wedge may be replaced by a constant penetration velocity equal to the resultant vertical velocity component of the equilibrium maximum pressure point on the wedge subsequent to q. This assumption is founded on the premise that the flow in the vicinity of the spray-root area of the wedge is the controlling factor in a determination of loads. Thus,

$$v_s = v_o + q\ell \cos\alpha \quad , \tag{35}$$

where v_o is the equilibrium penetration velocity associated with planing (see equation (1)). Substituting the right-hand side of equation (35) into equations (33) and (34), and then evaluating the derivatives with respect to q at equilibrium results in

$$(dZ_1)_q = \rho \frac{p_a}{\frac{\rho}{2} v_o^2} v_o \ell^2 \sin\alpha \cos\beta_a \, d\ell \tag{36}$$

and

$$(dZ_2)_q = \rho \frac{p_a}{\frac{\rho}{2} v_o^2} v_o \ell \frac{\cos^2\alpha}{\sin\alpha} (L_k \sec\alpha - \ell)\cos\beta_a \, d\ell \quad . \tag{37}$$

Finally, after considerable computation, Z_q is found from

$$Z_q = 2\int_0^{L_k\cos\alpha} (dZ_1)_q + 2\int_{L_k\cos\alpha}^{L_k\sec\alpha} (dZ_2)_q \quad , \tag{38}$$*

to be

$$Z_q = \frac{2}{3} \frac{Z_o L_k}{V_R \cos\tau_o} \left(\frac{V_R}{v_o}\right) (1 + \cos^2\alpha) \left(\frac{\cos\beta_a}{\cos\beta}\right) \quad . \tag{39}$$

In the derivation of equation (39), the following definition of the equilibrium Z-force has been used:

$$Z_o = p_a L_k C_p \cos\tau \quad . \tag{40}$$

---

* The factor 2 enters by the symmetry of slices on both sides of the planing body.

The significant physical considerations used in establishing the expression for Z_q are (1) the total lift on a planing body may be treated as a summation of effects which occur in sections normal to the stagnation line, (2) the average pressure coefficient is a geometrically determined constant which is independent of q, and (3) the resultant motion of the equilibrium maximum pressure point in sections normal to the stagnation line is assumed to determine the motion of the entire section.

M-MOMENT DERIVATIVES

In order to evaluate the required moment derivatives with the exception of M_q, an expression must be developed for the moment about the instantaneous leading edge of the wetted area in terms of the instantaneous wetted length, L', and the instantaneous Z-force. This expression will be based on the lift theory developed in this report and will be true for any purely translatory motion (i.e., $q = 0$).

It is necessary to establish expressions for the incremental moments, dM_1 and dM_2, about an axis through the leading edge of the wetted area and parallel to the y-axis, which are contributed by slices of the wetted portion of the planing body normal to the stagnation line. Referring to Figure 18, these expressions are as follows:

$$dM_1 = (0.4\ell \tan\alpha \sin\alpha + \ell\cos\alpha)dZ_1 \qquad (0 < \ell < L'\cos\alpha) \qquad (41)$$

and

$$dM_2 = (0.6\ell \cos\alpha + 0.4\ L')dZ_2 \qquad (L'\cos\alpha < \ell < L'\sec\alpha) \quad . \quad (42)$$

The quantities multiplying dZ_1 and dZ_2 are respectively the distances from the moment axis to the center of pressure in the normal sections for $(0 < \ell < L'\cos\alpha)$ and $(L'\cos\alpha < \ell < L'\sec\alpha)$. From Figure 12, the center-of-pressure location on the wedges in these normal sections was found to be approximately 0.6 C_s' (see Figure 18) for values of β_a from 20° to 40°. Little significant variation from this value is expected for other reasonable values of β_a. The total moment, M, is

$$M = \int_0^{L'\cos\alpha} dM_1 + \int_{L'\cos\alpha}^{L'\sec\alpha} dM_2 \quad . \qquad (43)$$

Substituting the values of dZ_1 and dZ_2 obtained from equations (33) and (34) into equations (41) and (42), inserting the result into equation (43), and integrating gives

$$M = \frac{2}{3} F_1(\alpha) L' Z \qquad (44)$$

as the expression for M in terms of the instantaneous wetted length and Z-force, where

$$F_1(\alpha) = \cos^2\alpha(0.4 \sin^2\alpha + \cos^2\alpha) + \csc^2\alpha(0.6 \cos^6\alpha - 0.3 \cos^4\alpha - 1.2 \cos^2\alpha + 0.9) \quad . \quad (45)$$

The variation of $F_1(\alpha)$ with α, the angle between the stagnation line and keel of the planing body, is shown in Figure 19. It is seen that the value of $F_1(\alpha) = 1$ is valid for all practical purposes; therefore,

$$M = \frac{2}{3} L' Z \quad . \tag{46}$$

This two-thirds value has been experimentally verified by some previous landing tests of Vee-bottom surfaces prior to chine immersion (Reference 11).

From equation (46), the moment derivatives M_z, M_τ, and M_w are easily obtained in terms of the corresponding Z-force derivatives and subsequently in terms of the equilibrium planing geometry and Z-force. These derivatives are discussed below:

The pitching moment change with change in depth, M_z, is expressed as

$$M_z = \frac{2}{3} L_k Z_z + \frac{2}{3} L'_z Z_o \quad , \tag{47}$$

which becomes, using equation (22) for L'_z,

$$M_z = \frac{2}{3} L_k Z_z + \frac{2Z_o}{3 \sin\tau_o} \quad . \tag{48}$$

Equation (24) is used to express Z_z in terms of the equilibrium Z-force, Z_o. Thus,

$$M_z = \frac{2Z_o}{\sin\tau_o} \quad . \tag{49}$$

The pitching moment change with change in trim angle, M_τ, is given by

$$M_\tau = \frac{2}{3} L_k Z_\tau + \frac{2}{3} Z_o L'_\tau \quad . \tag{50}$$

As previously shown (page 21), $L'_\tau = 0$. Finally, using equation (28) to obtain Z_τ in terms of Z_o results in

$$M_\tau = \frac{3.6}{\sin 2\tau_o} L_k Z_o \quad . \tag{51}$$

The pitching moment change with change in vertical velocity, M_w, is given by

$$M_w = \frac{2}{3} L_k Z_w + \frac{2}{3} Z_o L'_w \quad . \tag{52}$$

At equilibrium, $L'_w = 0$. Z_w is obtained in terms of Z_o by using equation (32). Hence,

$$M_w = \frac{4L_k}{3V_R \tan\tau_o} Z_o \quad . \tag{53}$$

The pitching moment change with change in angular velocity, M_q, must be treated in a manner analogous to Z_q inasmuch as equation (46) is no longer valid for rotational motion. Knowing this, the expressions for dM_1 and dM_2 must be first differentiated with respect to q and then integrated over the wetted area to obtain M_q.

The following derivatives may be obtained from equations (41) and (42):

$$(dM_1)_q = (0.4\ell \tan\alpha \sin\alpha + \ell \cos\alpha)(dZ_1)_q \tag{54}$$

$$(dM_2)_q = (0.6\ell \cos\alpha + 0.4\, L_k)(dZ_2)_q \quad . \tag{55}$$

Finally, after the expressions for $(dZ_1)_q$ and $(dZ_2)_q$ evaluated at equilibrium are inserted into equations (54) and (55) and the resultant expressions are integrated over the wetted area, the result is

$$M_q = \frac{2_o L_k^2}{3V_R \cos\tau_o} \left(\frac{V_R}{v_o}\right) F_2(\alpha) \left(\frac{\cos\beta_a}{\cos\beta}\right) \quad , \tag{56}$$

where

$$F_2(\alpha) = \csc^2\alpha[1.8 \cos^8\alpha + \cos^6\alpha(3 \sin^2\alpha - 0.8) + \cos^4\alpha(1.25 \sin^4\alpha - 2.4) + 1.4] \quad . \tag{57}$$

A plot of $F_1(\alpha)$ vs. α is shown on Figure 19.

REMARKS

A summary of all the stability derivatives derived above is presented in Table II. The following are believed to be the significant factors distinguishing this analysis from any other:

(1) With the exception of Z_τ and M_τ, the above derivatives have been expressed in terms of the theoretical equilibrium lift force, which can be obtained once the deadrise and trim angles of the body are known.

(2) The theory has allowed for the evaluation of all the derivatives with full cognizance being taken of the variation of C_L with the quantities z, w, τ, and q.

CONCLUDING REMARKS

A theory of the pressure distribution and load on a three-dimensional prismatic planing body has been developed in this report, subject to the usual assumptions regarding the flow about the body, which are:

(1) The fluid is incompressible and inviscid.

(2) The gravity forces may be considered negligible in comparison with the dynamic forces of the fluid.

The proposed theory treats the flow about the planing body in planes perpendicular to its stagnation line to be equivalent to the two-dimensional flow about an immersing wedge. In this way, the present study derives pressure distributions in sections of the body perpendicular to the stagnation line, and total loads acting on the body over a wide range of planing conditions. Additional special assumptions were required to treat the three-dimensional planing case in terms of a corresponding two-dimensional theory. These are:

(3) There exists, on the planing-body bottom, a stagnation line which is defined as the locus of points of maximum pressure.

(4) The flow along the stagnation line has a uniform velocity which is the component of the freestream velocity in the spatial direction of the stagnation line.

All the assumptions appear reasonable on the basis of the good agreement found between the theoretically predicted and measured maximum pressures and planing loads.

The results of this study are presented for the most part in graphical form since the theory of the two-dimensional penetrating wedge which was used is available in this form only. The graphs include theoretically determined variations of both the dimensionless maximum pressure, based on planing stagnation pressure, and the lift coefficient, based on wetted keel length, planing velocity, and fluid density, with the geometric planing parameters of trim and deadrise angles. The maximum pressure coefficient compares well with experimental data obtained from landing tests of planing bodies with deadrise angles of $22\frac{1}{2}^{\circ}$ and 30° over trim angles ranging from 0.2° to 30°. The variation of the theoretically predicted lift coefficients with body parameters shows good agreement with the measured variation over the ranges $10^{\circ} < \beta < 40^{\circ}$ and $2^{\circ} < \tau < 12^{\circ}$. The magnitudes of the theoretical lift coefficients are slightly greater than the measured ones. This may well be expected since the theory does not accurately reproduce the loss of pressure, or local load, which is believed to occur at the step of the planing body.

The results of the theory are in a generally applicable form as demonstrated by the development of stability derivatives which can be used in a linear porpoising analysis. The physical picture of the planing body afforded by this theory will be useful in future design and analysis work of planing bodies.

REFERENCES

1. Pierson, John D. *The Penetration of a Fluid Surface by a Wedge.* Stevens Institute of Technology, Experimental Towing Tank Report No. 381, July 1950. Sherman M. Fairchild Publication Fund Paper No. FF-3, Institute of the Aeronautical Sciences, New York.

2. Pierson, John D. and Leshnover, Samuel. *Study of the Flow, Pressures, and Loads Pertaining to Prismatic Vee-Planing Surfaces.* Stevens Institute of Technology, Experimental Towing Tank Report No. 382, May 1950. Sherman M. Fairchild Publication Fund Paper No. FF-2, Institute of the Aeronautical Sciences, New York.

3. Shoemaker, James M. *Tank Tests of Flat and V-Bottom Planing Surfaces.* NACA TN No. 509, November 1934, National Advisory Committee for Aeronautics, Washington, D.C.

4. Pierson, John D. *On the Pressure Distribution for a Wedge Penetrating a Fluid Surface.* Stevens Institute of Technology, Experimental Towing Tank Report No. 336, June 1948. Sherman M. Fairchild Publication Fund Paper No. 167, Institute of the Aeronautical Sciences, New York.

5. Pierson, John D. and Leshnover, Samuel. *An Analysis of the Fluid Flow in the Spray Root and Wake Regions of Flat Planing Surfaces.* Stevens Institute of Technology, Experimental Towing Tank Report No. 335, October 1948. Sherman M. Fairchild Publication Fund Paper No. 166, Institute of the Aeronautical Sciences, New York.

6. Wagner, Herbert. *Über Stoss-und Gleitvorgänge an der Oberfläche von Flüssigkeiten.* Z.f.a.M.M., Bd. 12, Heft 4, August 1932.

7. Smiley, Robert F. *A Study of Water Pressure Distribution During Landings with Special Reference to a Prismatic Model Having a Heavy Beam Loading and a 30° Angle of Deadrise.* NACA TN No. 2111, July 1950, National Advisory Committee for Aeronautics, Washington, D.C.

8. Smiley, Robert F. *Water-Pressure Distributions During Landings of a Prismatic Model Having an Angle of Deadrise of 22½° and Beam-Loading Coefficients of 0.48 and 0.97.* NACA TN No. 2816, November 1952, National Advisory Committee for Aeronautics, Washington, D.C.

9. Savitsky, Daniel. *Wetted Length and Center of Pressure of Vee-Step Planing Surfaces.* Stevens Institute of Technology, Experimental Towing Tank Report No. 378, September 1951. Sherman M. Fairchild Publication Fund Paper No. FF-6, Institute of the Aeronautical Sciences, New York.

10. Perring, W.G.A. and Glauert, H. *Stability on the Water of a Seaplane in the Planing Condition.* Aeronautical Research Committee Reports and Memoranda No. 1493, His Majesty's Stationery Office, London, September 1932.

11. Milwitsky, Benjamin. *A Generalized Theoretical Investigation of the Hydrodynamic Pitching Moments Experienced by V-Bottom Seaplanes During Step-Landing Impacts and Comparisons with Experiment.* NACA TN No. 1630, June 1948, National Advisory Committee for Aeronautics, Washington, D.C.

APPENDIX A

REPORTS AND PAPERS COMPLETED TO DATE AT THE E.T.T. UNDER CONTRACT NO. N6onr-24704 WITH THE OFFICE OF NAVAL RESEARCH

ON PLANING SURFACES

WETTED AREAS, LOADS, AND PRESSURES

Korvin-Kroukovsky, B.V.; Savitsky, Daniel; and Lehman, William F. *Wetted Area and Center of Pressure of Planing Surfaces.* Stevens Institute of Technology, Experimental Towing Tank Report No. 360, August 1949. Sherman M. Fairchild Publication Fund Paper No. 244, Institute of the Aeronautical Sciences, New York.

Pierson, John D. and Leshnover, Samuel. *Study of Flow, Pressures, and Loads Pertaining to Prismatic Vee-Planing Surfaces.* Stevens Institute of Technology, Experimental Towing Tank Report No. 382, May 1950. Sherman M. Fairchild Publication Fund Paper No. FF-2, Institute of the Aeronautical Sciences, New York.

Korvin-Kroukovsky, B.V. *Lift of Planing Surfaces.* Stevens Institute of Technology, Experimental Towing Tank Paper Published in the Reader's Forum Section of the Journal of Aeronautical Sciences, September 1950.

Savitsky, Daniel. *Wetted Length and Center of Pressure of Vee-Step Planing Surfaces.* Stevens Institute of Technology, Experimental Towing Tank Report No. 378, September 1951. Sherman M. Fairchild Publication Fund Paper No. FF-6, Institute of the Aeronautical Sciences, New York.

WAVE FORM IN VICINITY OF PLANING SURFACES

Korvin-Kroukovsky, B.V.; Savitsky, Daniel; and Lehman, William F. *Wave Contours in the Wake of a 20° Deadrise Planing Surface.* Stevens Institute of Technology, Experimental Towing Tank Report No. 337, June 1948. Sherman M. Fairchild Publication Fund Paper No. 168, Institute of the Aeronautical Sciences, New York.

Pierson, John D. and Leshnover, Samuel. *An Analysis of the Fluid Flow in the Spray Root and Wake Regions of Flat Planing Surfaces.* Stevens Institute of Technology, Experimental Towing Tank Report No. 335, October 1948. Sherman M. Fairchild Publication Fund Paper No. 166, Institute of the Aeronautical Sciences, New York.

Korvin-Kroukovsky, B.V.; Savitsky, Daniel; and Lehman, William F. *Wave Contours in the Wake of a 10° Deadrise Planing Surface.* Stevens Institute of Technology, Experimental Towing Tank Report No. 344, November 1948. Sherman M. Fairchild Publication Fund Paper No. 170, Institute of the Aeronautical Sciences, New York.

Korvin-Kroukovsky, B.V.; Savitsky, Daniel; and Lehman, William F. *Wave Profile of a Vee-Planing Surface, Including Test Data on a 30° Deadrise Surface.* Stevens Institute of Technology, Experimental Towing Tank Report No. 339, April 1949. Sherman M. Fairchild Publication Fund Paper No. 229, Institute of the Aeronautical Sciences, New York.

ON THE IMMERSING WEDGE

Pierson, John D. *On the Pressure Distribution for a Wedge Penetrating a Fluid Surface.* Stevens Institute of Technology, Experimental Towing Tank Report No. 336, June 1948. Sherman M. Fairchild Publication Fund Paper No. 167, Institute of the Aeronautical Sciences, New York.

Korvin-Kroukovsky, B.V. and Chabrow, Faye R. *The Discontinuous Fluid Flow Past an Immersed Wedge.* Stevens Institute of Technology, Experimental Towing Tank Report No. 334, October 1948. Sherman M. Fairchild Publication Fund Paper No. 169, Institute of the Aeronautical Sciences, New York.

Pierson, John D. *On the Penetration of a Fluid Surface by a Wedge.* Stevens Institute of Technology, Experimental Towing Tank Report No. 381, July 1950. Sherman M. Fairchild Publication Fund Paper No. FF-3, Institute of the Aeronautical Sciences, New York.

Pierson, John D. *On the Virtual Mass of Water Associated with an Immersing Wedge.* Stevens Institute of Technology, Experimental Towing Tank Paper Published in the Readers' Forum Section of the Journal of Aeronautical Sciences, June 1951.

APPENDIX B

DERIVATION OF THE ASSOCIATED DEADRISE ANGLE IN TERMS OF THE PLANING BODY GEOMETRY

The associated deadrise angle has been defined in the text as the deadrise angle of the two-dimensional immersing wedge associated with the passage of a planing body through a plane which is stationary in space and oriented normal to the stagnation line of the body. In the present derivation, this is the angle made between the line of intersection of the stationary plane and the body surface, and this plane and the water surface.

The task of deriving an expression for the associated deadrise angle in terms of the trim and deadrise angles of the planing body therefore becomes simply a problem in geometry. The axis system is fixed at the leading edge of the wetted area, with the x-axis positive in the di-

rection of motion, the z-axis positive vertically downward, and the y-axis positive to starboard. With the direction cosines of the upward direction of the stagnation line on the starboard side of the planing body and the keel line denoted by $(\lambda_1, \mu_1, \nu_1)$ and $(\lambda_2, \mu_2, \nu_2)$, respectively, the equation of the planing surface bottom on the starboard side may be written as

$$\begin{vmatrix} \mu_1 & \nu_1 \\ \mu_2 & \nu_2 \end{vmatrix} x + \begin{vmatrix} \nu_1 & \lambda_1 \\ \nu_2 & \lambda_2 \end{vmatrix} y + \begin{vmatrix} \lambda_1 & \mu_1 \\ \lambda_2 & \mu_2 \end{vmatrix} z = 0 \quad . \tag{B-1}$$

The equation of the plane normal to the stagnation line on the starboard side and passing through the origin is

$$\lambda_1 x + \mu_1 y + \nu_1 z = 0 \tag{B-2}$$

and the equation of the water surface is, of course,

$$z = 0 \quad . \tag{B-3}$$

A set of direction numbers for the upward direction of the line of intersection between the plane normal to the stagnation line and the plane of the bottom is obtained from equations (B-1) and (B-2) to be

$$\begin{vmatrix} -\mu_1 & 0 & \nu_1 \\ \nu_1 & \lambda_1 & \mu_1 \\ \nu_2 & \lambda_2 & \mu_2 \end{vmatrix} , \begin{vmatrix} \lambda_1 & -\nu_1 & 0 \\ \nu_1 & \lambda_1 & \mu_1 \\ \nu_2 & \lambda_2 & \mu_2 \end{vmatrix} , \begin{vmatrix} 0 & \mu_1 & -\lambda_1 \\ \nu_1 & \lambda_1 & \mu_1 \\ \nu_2 & \lambda_2 & \mu_2 \end{vmatrix} . \tag{B-4}$$

The starboard-side direction of the line of intersection between the normal plane and the plane of the water surface has the direction numbers

$$(\mu_1 \ , \ -\lambda_1 \ , \ 0) \quad . \tag{B-5}$$

With the direction cosines associated with the direction numbers in (B-4) and (B-5) denoted by $(\alpha_1, \beta_1, \gamma_1)$ and $(\alpha_2, \beta_2, \gamma_2)$, respectively, then

$$\cos\beta_a = \alpha_1\alpha_2 + \beta_1\beta_2 + \gamma_1\gamma_2 \quad , \tag{B-6}$$

where β_a is the angle between the lines of intersection of the normal plane with the body and with the water surface and is therefore the desired associated deadrise angle. Using the expressions given by equations (13a), (13b), and (13c) of Reference 2, corrected to the starboard side for $(\lambda_1, \mu_1, \nu_1)$, and using $(\cos\tau, 0, -\sin\tau)$ for $(\lambda_2, \mu_2, \nu_2)$ results in

$$\alpha_1 = \frac{(K - \sin^2\beta)/\sin\beta}{[(1/\sin^2\tau) + (K^2/\sin^2\beta\cos^2\tau)]^{1/2}}$$

$$\beta_1 = \frac{\cos\beta/\sin\tau}{[(1/\sin^2\tau) + (K^2/\sin^2\beta\ \cos^2\tau)]^{1/2}}$$

$$\gamma_1 = \frac{-(K\ \tan\tau/\sin\beta + \sin\beta/\tan\tau)}{[(1/\sin^2\tau) + (K^2/\sin^2\beta\ \cos^2\tau)]^{1/2}}$$

$$\alpha_2 = \frac{K\ \tan\tau/\tan\beta}{[(K\ \tan\tau/\tan\beta)^2 + (K\ \tan\tau\ \sin\tau)^2 + \cos^2\tau + 2K\ \sin^2\tau]^{1/2}}$$

$$\beta_2 = \frac{-(\cos\tau + K\ \tan\tau\ \sin\tau)}{[(K\ \tan\tau/\tan\beta)^2 + (K\ \tan\tau\ \sin\tau)^2 + \cos^2\tau + 2K\ \sin^2\tau]^{1/2}}$$

$$\gamma_2 = 0 \quad ,$$

where τ and β are respectively the trim and deadrise angles of the planing body, and the quantity K is a function of deadrise angle, defined in Reference 2 as the ratio of two distances -- one from the centerline of an immersing wedge to the maximum pressure point, and the other from this centerline to the still water intersection point, respectively. This definition shows K to be a function of the planing body deadrise β since the immersing wedge in Reference 2 has the same deadrise as the planing body. Shown in Figure B-1 (page 59) is a curve of K vs. wedge deadrise angle obtained from the results of Reference 1. The curve may be used to obtain K for the purposes of calculating α_1, β_1,...,γ_2 above if the wedge deadrise angle in Figure B-1 is taken as β.

APPENDIX C

DERIVATION OF EQUATION (1)

The reader is referred to Figure 1 for the following development of the penetration velocity of the associated immersing wedge since, in this Figure, true view dimensions of the planing body are clearly represented. The derivation is a result of the mathematical statement of the physical condition discussed in the text, namely, to an observer fixed in a stationary plane taken normal to the stagnation line of the planing body, the motion of this stagnation line in the plane must be equivalent to the motion of the traveling maximum pressure point of the immersing two-dimensional wedge which represents the planing surface.

In Figure 1, the distance that the body must travel in the x-direction in order that the stagnation line pass completely through the stationary plane is $OK_1 \cos\tau$. At the time when the point S_1 on the step enters the stationary plane, this plane intersects the extended keel line

at K_1. It can be verified that the length S_1K_1 measured in the plane of the planing surface bottom is

$$S_1K_1 = \frac{C_s}{\cos\beta \cos\alpha} \quad , \tag{C-1}$$

where C_s is the labeled distance from the centerline plane to the intersection of the stagnation line and step, and where α is the angle between the keel and stagnation line of the planing surface. Also,

$$OK_1 = \frac{S_1K_1}{\sin\alpha} \quad . \tag{C-2}$$

The time, t, taken by the body to traverse the distance $OK_1 \cos\tau$ at the planing velocity V_R is

$$t = \frac{OK_1 \cos\tau}{V_R} \quad . \tag{C-3}$$

To an observer fixed in the stationary plane, it then appears that the traveling maximum pressure point of the associated deadrise wedge is moving outboard along the wedge with velocity v', where

$$v' = \frac{S_1K_1}{t} \quad , \tag{C-4}$$

which, by (C-1), (C-2), and (C-3), is

$$v' = V_R \frac{\sin\alpha}{\cos\tau} \quad . \tag{C-5}$$

The remaining problem is to relate the penetration velocity, v_o, to this velocity outboard along the wedge. To this end, consideration will be given to the flow field of the immersing wedge of deadrise β_a in the stationary plane (Figure 2). In this Figure are labeled the analogous distances which appear in Figure 1, namely, y', C_s', and C_p', which are the distances from the centerline plane to the still water intersection, to the maximum pressure point, and to the spray root, respectively. Clearly, from this Figure,

$$v' = \frac{\dot{C}_s'}{\cos\beta_a} \quad , \tag{C-6}$$

where the dot indicates time differentiation.

The flow about an immersing wedge changes with time. However, this time variation of the flow is in reality a spatial expansion or growth of a single flow pattern. Hence, if certain relations between distances in the flow pattern hold true for one time, they are invariant for all times.

This condition, which may be termed a "similarity of flow condition," gives

$$C_p' = e y' \quad , \tag{C-7}$$

or, equivalently,

$$\dot{C}_p' = \frac{e v_o}{\tan\beta_a} \quad ; \tag{C-8}$$

it also gives

$$C_s' = K y' \quad . \tag{C-9}$$

Here, e and K are constants for any given deadrise angle. It will be shown, however, that e disappears in the succeeding development so that the final equation depends on K only.

The curve of Figure B-1 shows K vs. wedge deadrise angle. This curve may be used to obtain K vs. β_a if the wedge deadrise angle in this Figure is taken as β_a. It is noted that Figure B-1 was also used to obtain K vs. β, the planing body deadrise angle (see APPENDIX B, page 32). These two uses are possible only if it is assumed that the physical flow pictures in planes normal to the keel and normal to the stagnation line both are well represented as an immersing wedge.

Combining equations (C-7) and (C-9) and differentiating with respect to time gives

$$\dot{C}_s' = \frac{K}{e} \dot{C}_p' \quad , \tag{C-10}$$

which, when substituted into equation (C-6), results in

$$v' = \frac{K}{e} \frac{\dot{C}_p'}{\cos\beta_a} \quad . \tag{C-11}$$

Finally, if the right-hand side of equation (C-8) is used for $\dot{C}_p'$ and the right-hand sides of equations (C-5) and (C-11) are equated, the relation

$$v_o = \frac{\sin\beta_a \sin\alpha}{K \cos\tau} V_R \tag{C-12}$$

is obtained. It should be remembered from equation (C-9) that, here, K is considered as a function of β_a. For computational purposes, use is made of the following relation for $\tan\alpha$, which was obtained from equation (15) of Reference 2:

$$\tan\alpha = \frac{K \tan\tau}{\sin\beta} \quad . \tag{C-13}$$

Curves of v_o/V_R vs. τ with β_a as parameter appear on Figure 8.

APPENDIX D

DEVELOPMENT OF THE TRANSFORMATION EQUATIONS WHICH RELATE THE "STANDARD PORPOISING STABILITY DERIVATIVES" TO THOSE DERIVED IN THIS REPORT

In this study, "standard porpoising stability derivatives" are defined as those hydrodynamic force and moment derivatives of use in a linear porpoising stability analysis and derived from motions of, and about, the center of gravity of the planing body. These differ from the stability derivatives previously considered in the body of this report in that the latter are derived from motions of, and about, the leading edge of the wetted area of the planing body.

The two axis systems which delineate the above reference systems are shown in Figure 17. They are the space-fixed (x^*, z^*) axes and the body-fixed (x, z) axes. The latter are fixed in the planing body at the equilibrium point of intersection of the keel with the undisturbed water surface and are fixed in orientation. The planing body is shown in Figure 17a in its equilibrium planing condition, and in Figure 17b in an arbitrary perturbed state, where the body has been displaced and rotated about the C.G. In Figure 17b, the coordinate system fixed at the initial leading edge of the wetted area is displaced distances x and z from its initial state (denoted by 0), and the center of gravity is displaced from its initial state by distances x^*_{CG} and z^*_{CG}. The relations between these displacements, with the effect of a change in pitch angle about the center of gravity taken into account, are

$$x = x^*_{CG} + b(\sin\theta - \sin\theta_o) + a(\cos\theta - \cos\theta_o) \qquad \text{(D-1)}$$

$$z = z^*_{CG} + b(\cos\theta - \cos\theta_o) - a(\sin\theta - \sin\theta_o) \quad , \qquad \text{(D-2)}$$

where the distances a and b are respectively the perpendicular distance from the C.G. to the perpendicular to the keel at the point 0, and the perpendicular distance from the C.G. to the keel (note Figure 17). The first terms on the right-hand side of (D-1) and (D-2) are the changes in x and z due to pure displacement of the C.G.; the remaining terms are the changes in x and z due to pure rotation about the C.G.

Equations (D-1) and (D-2) may be differentiated to give the relations between velocities in the two systems. Furthermore, since the angles and angular rates of the two systems are identical, the resulting equations relating forces, moments, displacements, and velocities between the two systems are:

$$M - aN - \frac{zN}{\sin\tau} = M^* \qquad \text{(D-3)}$$

$$Z = Z^* \tag{D-4}$$

$$x = x^*_{CG} + b(\sin\theta - \sin\theta_o) + a(\cos\theta - \cos\theta_o) \tag{D-5}$$

$$z = z^*_{CG} + b(\cos\theta - \cos\theta_o) - a(\sin\theta - \sin\theta_o) \tag{D-6}$$

$$u = u^*_{CG} + bq^*\cos\theta - aq^*\sin\theta \tag{D-7}$$

$$w = w^*_{CG} - bq^*\sin\theta - aq^*\cos\theta \tag{D-8}$$

$$\tau = \theta \tag{D-9}$$

$$q = q^* \quad , \tag{D-10}$$

where

M is the moment about the instantaneous position of the leading edge of the wetted area;

M^* is the moment about the C.G.;

N is the resultant force normal to the keel;

q^*, q are the pitching angular velocities of the body about the C.G. and the origin of the (x,z) coordinate system, respectively;

u, w are velocities of the center of the (x,z) coordinate system relative to the point 0;

u^*_{CG}, w^*_{CG} are velocities of the C.G. along the x^* and z^* coordinate axes, respectively;

$Z^* = Z$ is the vertical force;

$\tau = \theta$ is the trim angle of the body.

In a linear analysis, it is permissible to replace the normal force N by the vertical force Z. This substitution is made in the following development.

Consider the following functional relations:

$$Z^* = Z(x,\ z,\ u,\ w,\ \tau,\ q)$$

$$M^* = M^*(x,\ z,\ u,\ w,\ \tau,\ q) \quad .$$

After applying the "chain rule" of partial differentiation, equations (D-3) through (D-10) are used to arrive at the following resultant expressions:

$$Z^*_{z^*_{CG}} = Z_z$$

$$Z^*_{w^*_{CG}} = Z_w$$

$$Z^*_{\theta} = Z_{\tau} - Z_z(b \sin\theta_o + a \cos\theta_o)$$

$$Z^*_{q^*} = Z_q - Z_u(-b \cos\theta_o + a \sin\theta_o) - Z_w(b \sin\theta_o + a \cos\theta_o)$$

$$M^*_{z^*_{CG}} = \left(M_z - aZ_z - \frac{Z}{\sin\tau_o}\right)$$

$$M^*_{w^*_{CG}} = (M_w - aZ_w)$$

$$M^*_{\theta} = M_{\tau} - aZ_{\tau} - \left(M_z - aZ_z - \frac{Z}{\sin\tau_o}\right)(b \sin\theta_o + a \cos\theta_o)$$

$$M^*_{q^*} = M_q - aZ_q - (M_u - aZ_u)(-b \cos\theta_o + a \sin\theta_o) - (M_w - aZ_w)(b \sin\theta_o + a \cos\theta_o).$$

These are the transformation equations which give the stability derivatives in the (x^*, z^*) coordinate system in terms of those derived in the text, namely, those in the (x, z) coordinate system.

TABLE I

TABULATION OF TEST DATA AND RESULTS

TEST PARAMETERS		TEST RESULTS		
Trim Angle, τ, deg.	Load, Δ, lb.	Wetted Length, L_k, beams	Wetted Width, $2C_p$, beams	Lift Coefficient, C_L
$\beta = 10^\circ$		V_R = 24.7 ft./sec.		
2	2.40	0.93	0.64	0.00837
	2.40	0.98	0.64	0.00769
	3.40	1.19	0.76	0.00726
	3.40	1.12	0.74	0.00817
4	4.91	0.50	0.62	0.0592
	4.91	0.48	0.64	0.0642
	5.91	0.58	0.72	0.0531
	5.91	0.58	0.76	0.0531
6	4.92	0.36	0.64	0.1145
	4.92	0.38	0.60	0.1007
	4.92	0.36	0.62	0.1145
	6.92	0.49	0.74	0.0871
	6.92	0.48	0.74	0.0904
	6.92	0.42	0.70	0.1187
	6.92	0.46	0.76	0.0988
8	4.93	0.22	0.50	0.3102
	4.93	0.22	0.52	0.3102
	6.93	0.30	0.66	0.2264
	6.93	0.35	0.70	0.1732
	6.93	0.35	0.70	0.1732
	6.93	0.34	0.66	0.1811
	9.93	0.36	0.78	0.2311
10	5.94	0.29	0.74	0.2148
	5.94	0.23	0.58	0.3364
	5.94	0.24	0.60	0.3153
	6.94	0.30	0.64	0.2305
	6.94	0.30	0.64	0.2305
12	4.95	0.18	0.50	0.4670
	6.95	0.20	0.48	0.5133
	6.95	0.20	0.42	0.5133
$\beta = 20^\circ$		V_R = 24.6 ft./sec.		
2	1.90	2.13	0.58	0.00128
	1.90	2.12	0.58	0.00129
4	1.90	0.80	0.44	0.00907
	2.90	0.92	0.54	0.0104
	2.90	0.92	0.48	0.0104
6	3.90	0.59	0.46	0.0336
	4.90	0.68	0.54	0.0325
8	4.90	0.44	0.66	0.0766
	4.90	0.46	0.48	0.0702
	4.90	0.43	0.46	0.0844
	3.90	0.40	0.42	0.0748
12	2.90	0.21	0.30	0.200
	2.90	0.19	0.30	0.250
	3.90	0.23	0.36	0.225
$\beta = 30^\circ$		V_R = 24.6 ft./sec.		
2	1.85	3.20	0.52	0.000552
	1.85	3.23	0.52	0.000543
	3.85	4.42	0.56	0.000657
	3.85	4.54	0.72	0.000572
	1.85	3.24	0.56	0.000566
	3.85	4.41	0.72	0.000657
4	3.85	1.76	0.58	0.00381
	3.85	1.76	0.56	0.00381
	3.85	1.76	0.59	0.00381
	1.85	1.27	0.40	0.00352
	1.85	1.27	0.40	0.00352
6	3.85	1.00	0.46	0.0118
	3.85	1.02	0.46	0.0113
	3.85	1.02	0.46	0.0113
	5.85	1.26	0.56	0.0113
	5.85	1.24	0.58	0.0118

TABLE I (cont'd.)

TEST PARAMETERS		TEST RESULTS		
Trim Angle, τ, deg.	Load, Δ, lb.	Wetted Length, L_k, beams	Wetted Width, $2C_p$, beams	Lift Coefficient, C_L
	$\beta = 30^\circ$	(cont'd.)	V_R = 24.6 ft./sec.	
8	5.85	0.80	0.52	0.0281
	5.85	0.78	0.50	0.0295
	3.85	0.63	0.40	0.0298
	3.85	0.62	0.40	0.0306
10	5.85	0.61	0.46	0.0482
	5.85	0.62	0.48	0.0463
	7.85	0.73	0.56	0.0451
	7.85	0.78	0.56	0.0396
12	7.85	0.52	0.52	0.0889
	7.85	0.53	0.52	0.0854
	5.85	0.45	0.44	0.0898
	5.85	0.45	0.46	0.0898

TABLE II

SUMMARY TABLE OF THE CALCULATED STABILITY DERIVATIVES

DERIVATIVE	VALUE IN TERMS OF EQUILIBRIUM Z-FORCE
	Z-Force Derivatives
Z_z	$\frac{2}{L_k \sin\tau_o} Z_o$
Z_τ	$\frac{5.4}{\sin 2\tau_o} Z_o$
Z_w	$\frac{2}{V_R \tan\tau_o} Z_o$
Z_q	$\frac{2L_k}{3V_R \cos\tau_o} \left(\frac{\cos\beta_a}{\cos\beta}\right) \left(\frac{V_R}{v_o}\right) (1 + \cos^2\alpha) Z_o$
	M-Moment Derivatives
M_z	$\frac{2}{\sin\tau_o} Z_o$
M_τ	$\frac{3.6 L_k}{\sin 2\tau_o} Z_o$
M_w	$\frac{4 L_k}{3V_R \tan\tau_o} Z_o$
M_q	$\frac{L_k{}^2 F_2(\alpha)}{3V_R \cos\tau_o} \left(\frac{V_R}{v_o}\right) \left(\frac{\cos\beta_a}{\cos\beta}\right) Z_o$

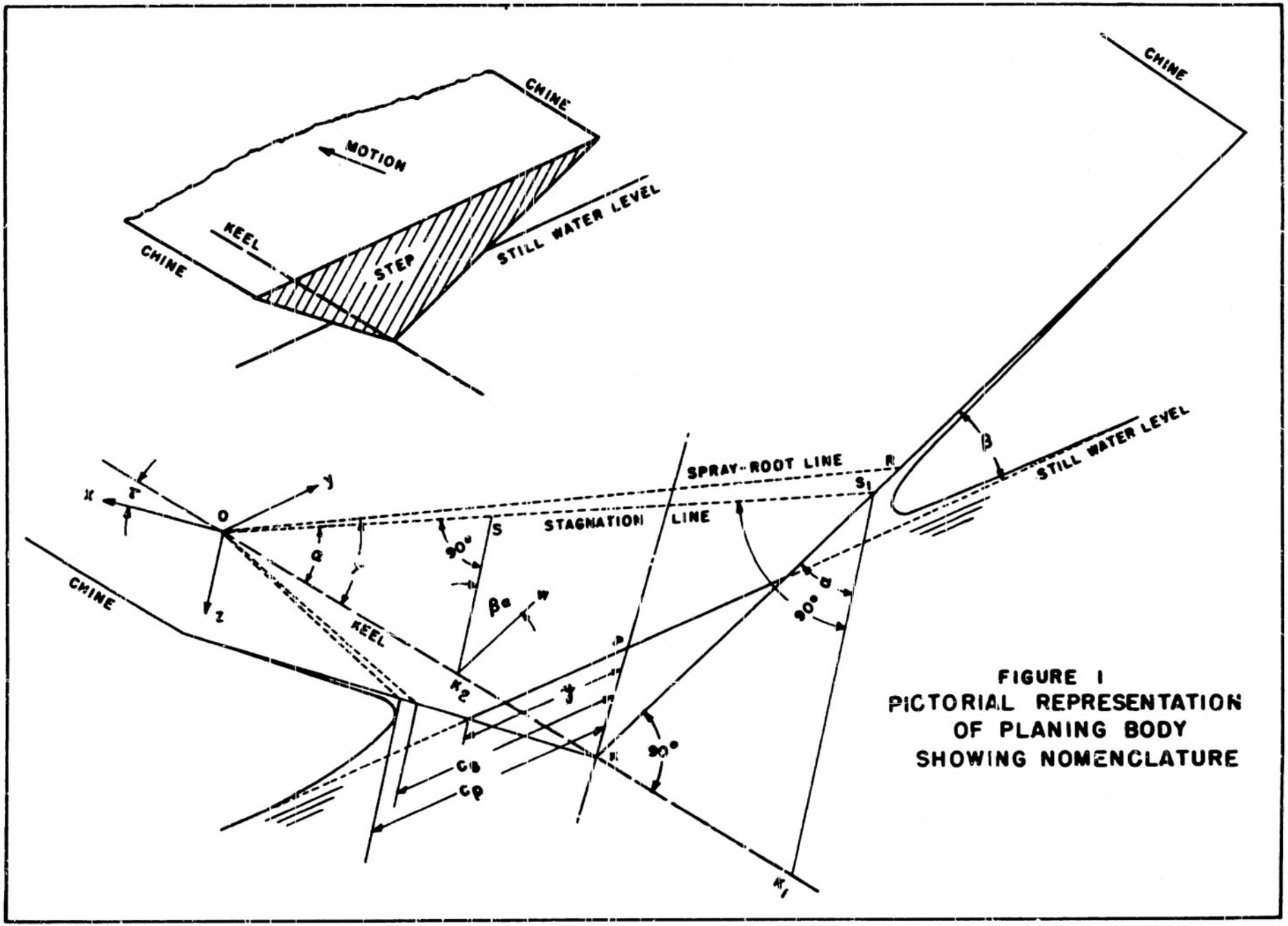

FIGURE 1
PICTORIAL REPRESENTATION
OF PLANING BODY
SHOWING NOMENCLATURE

FIGURE 2

THE IMMERSING WEDGE AS VIEWED IN THE STATIONARY PLANE

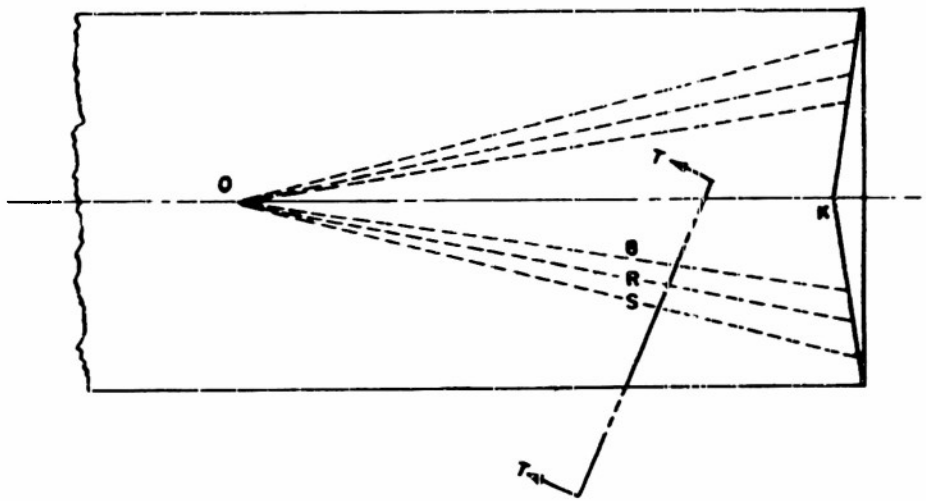

$\overline{OK}$ = KEEL LINE

$\overline{OB}$ = LEVEL WATER LINE

$\overline{OR}$ = STAGNATION LINE

$\overline{OS}$ = SPRAY-ROOT LINE

$\overline{TT}$ = TRACE OF THE STATIONARY PLANE INTERSECTION WITH THE BODY

T-T = SECTION PERPENDICULAR TO STAGNATION LINE

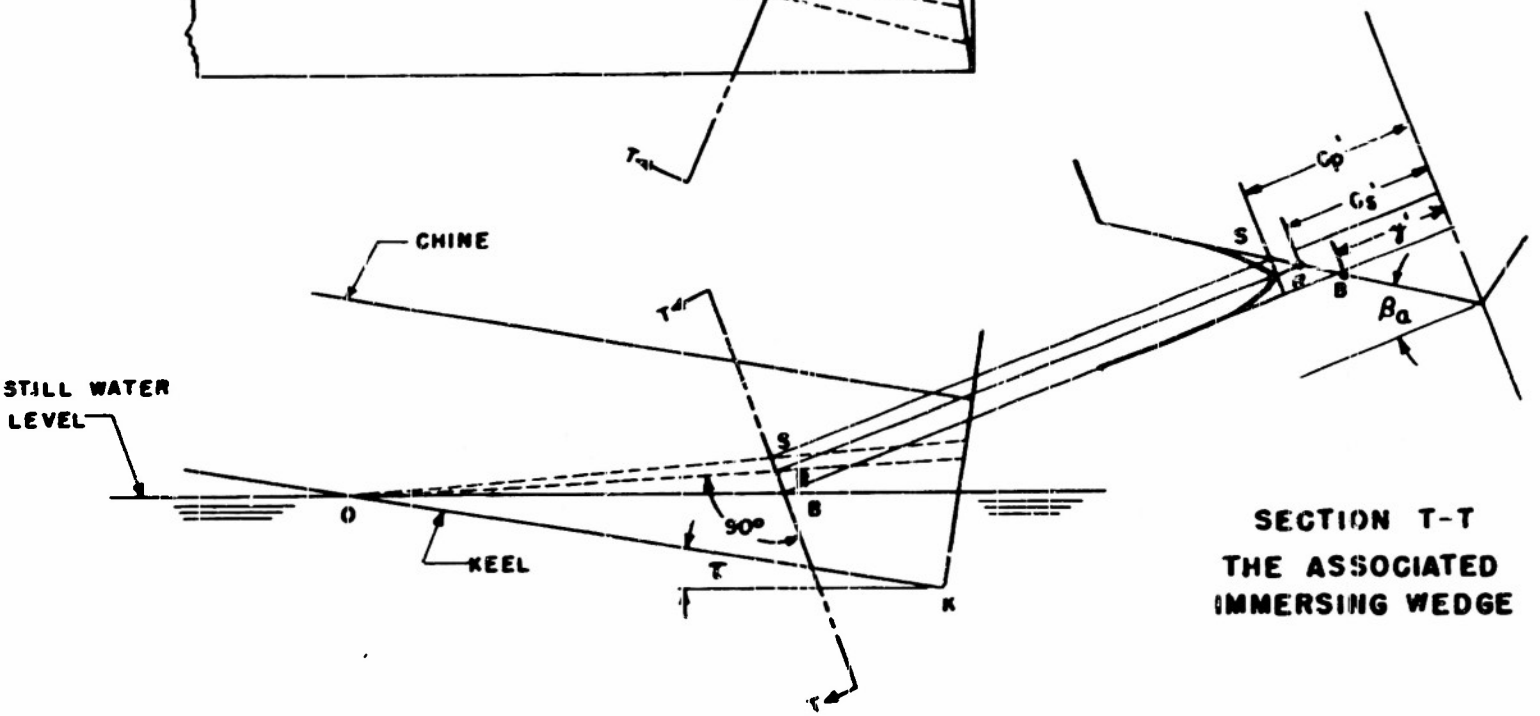

SECTION T-T

THE ASSOCIATED IMMERSING WEDGE

FIGURE 3

VARIATION OF ASSOCIATED WEDGE DEADRISE ANGLE WITH PLANING BODY DEADRISE AND TRIM ANGLES

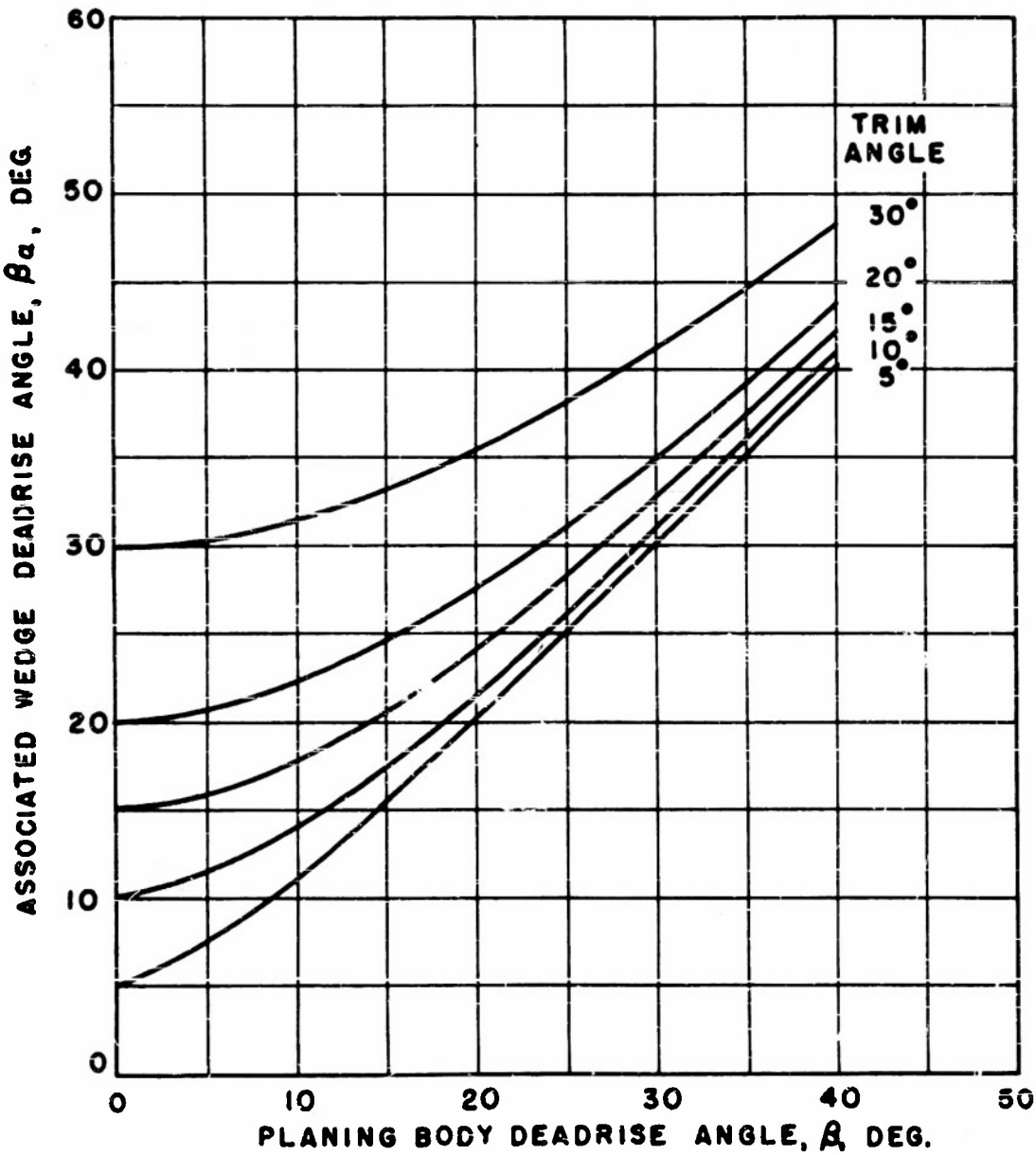

FIGURE 4

PHOTOGRAPH OF MODEL AND APPARATUS USED IN PLANING TESTS

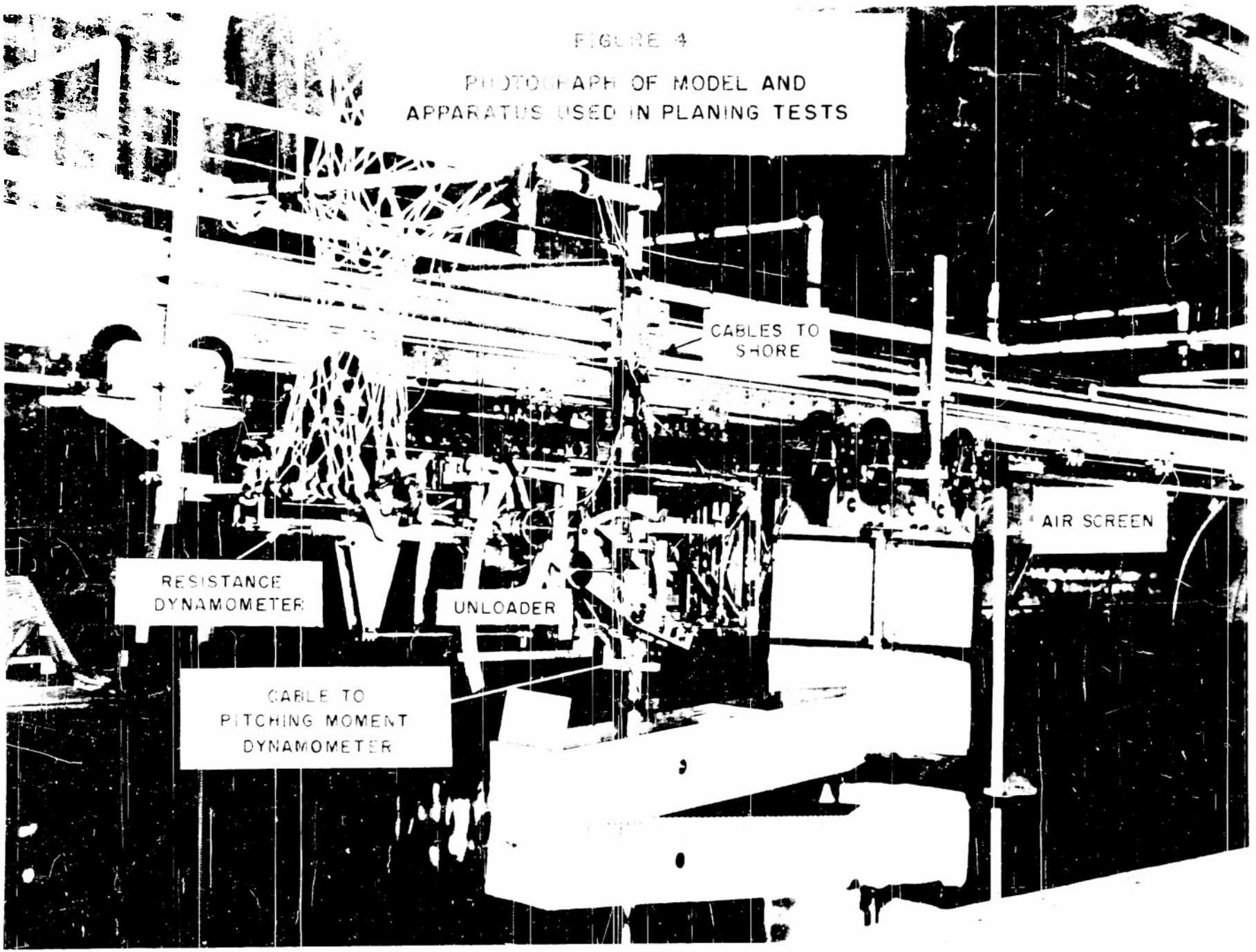

FIGURE 5

TYPICAL UNDERWATER PHOTOGRAPHS OF THE PLANING BODY

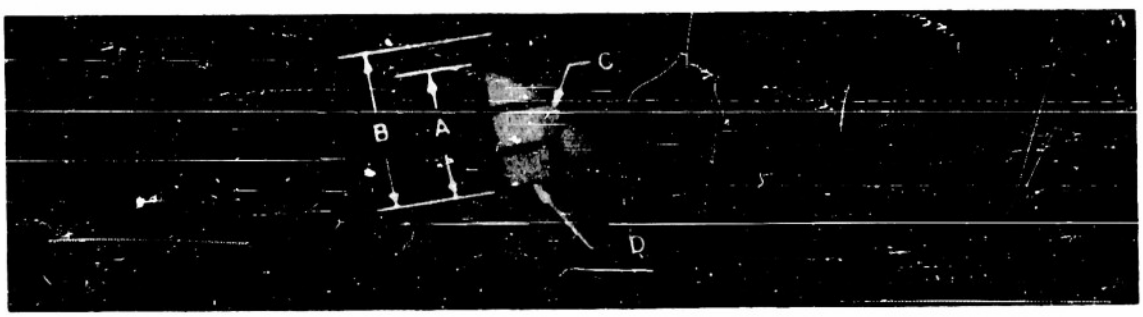

PLANING CONDITIONS

$\beta = 10^\circ$, $\tau = 12^\circ$, $\Delta = 7$ LB. $V_R = 24.66$ FT./SEC.

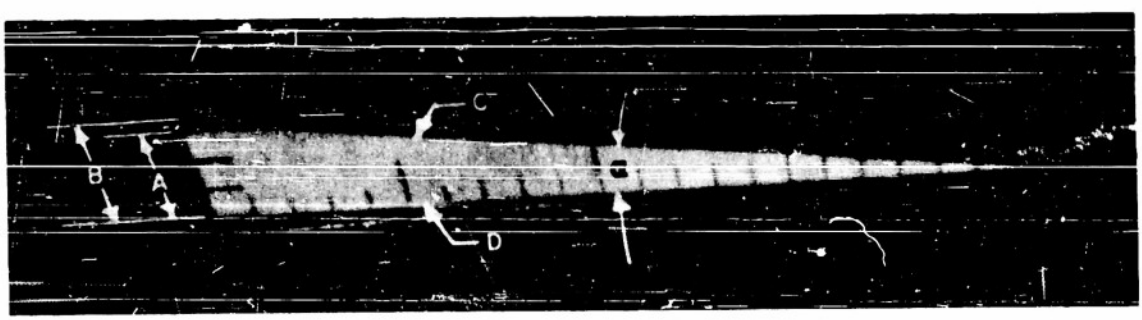

PLANING CONDITIONS

$\beta = 20^\circ$, $\tau = 2^\circ$, $\Delta = 2$ LB. $V_R = 24.50$ FT./SEC.

A = MEASURED VALUE OF C_p

B = PREDICTED VALUE OF C_p FROM EQ. (8) AND L_k

C = STAGNATION LINE

D = KEEL

FIGURE 6

COMPARISON OF EXPERIMENTAL AND THEORETICAL VALUES OF THE LIFT COEFFICIENT

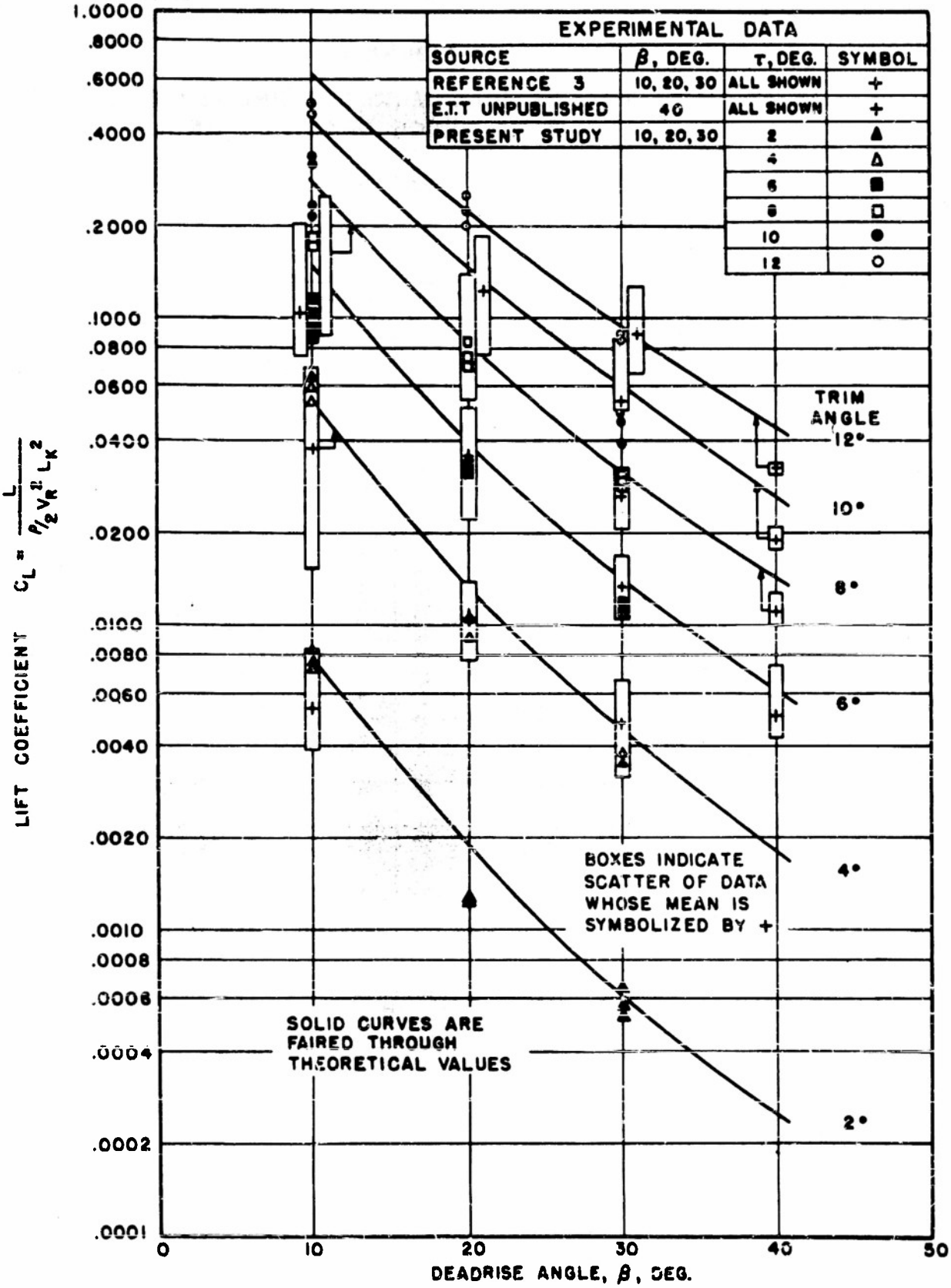

FIGURE 7

VARIATION OF THEORETICAL MAXIMUM PRESSURE COEFFICIENT WITH WEDGE DEADRISE ANGLE

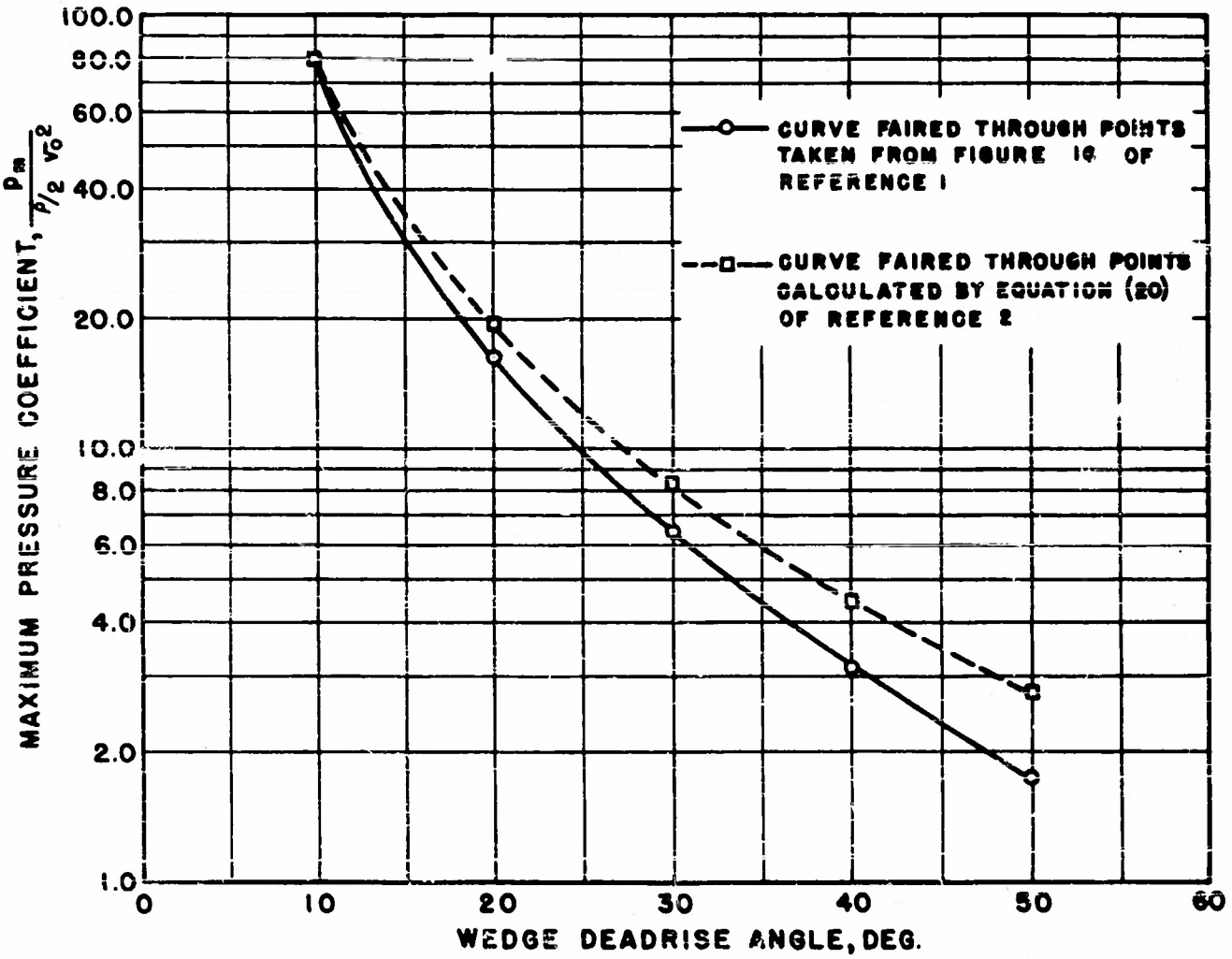

FIGURE 8

VARIATION OF $\frac{V_o}{V_R}$ RATIO

WITH PLANING BODY DEADRISE AND TRIM ANGLES

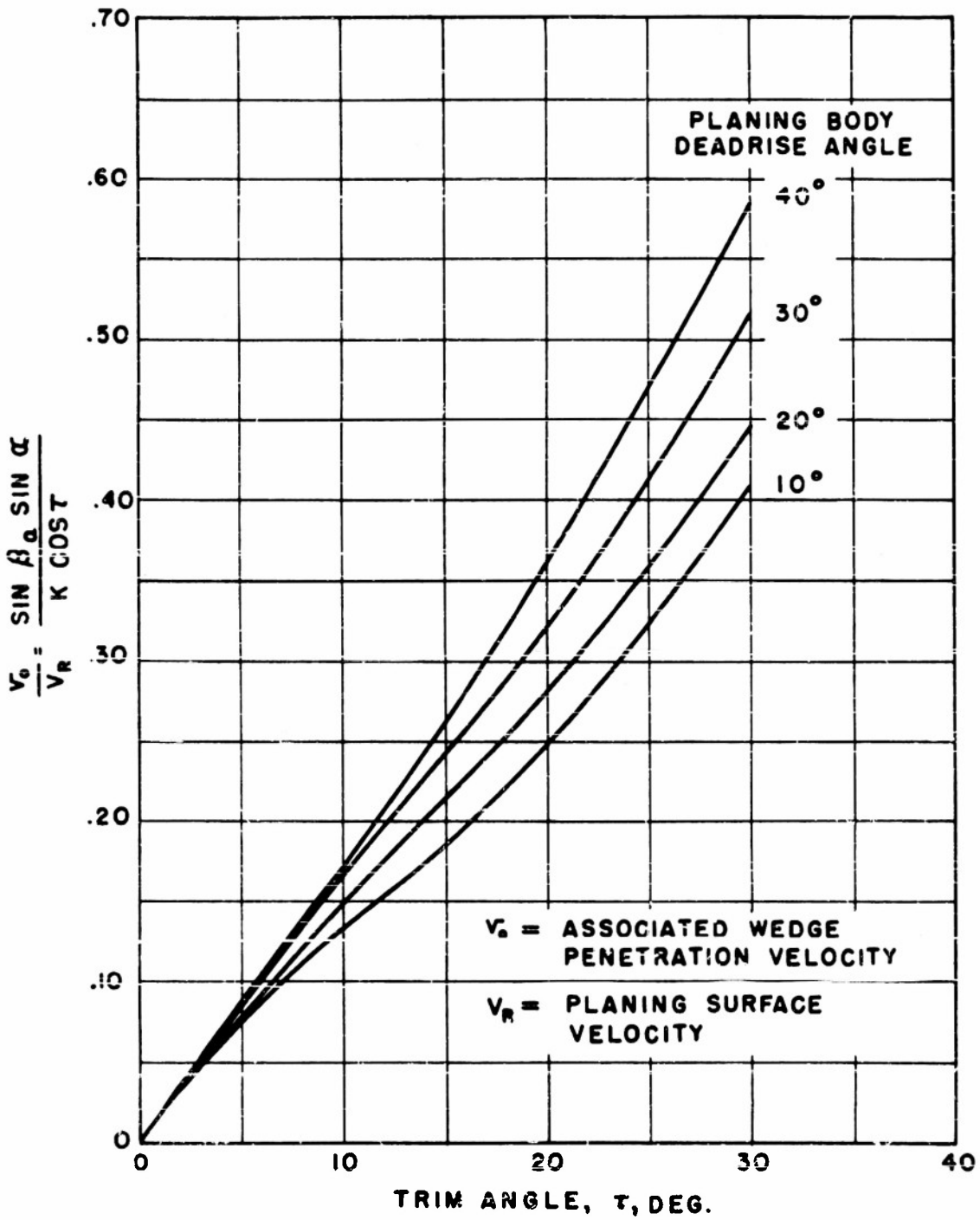

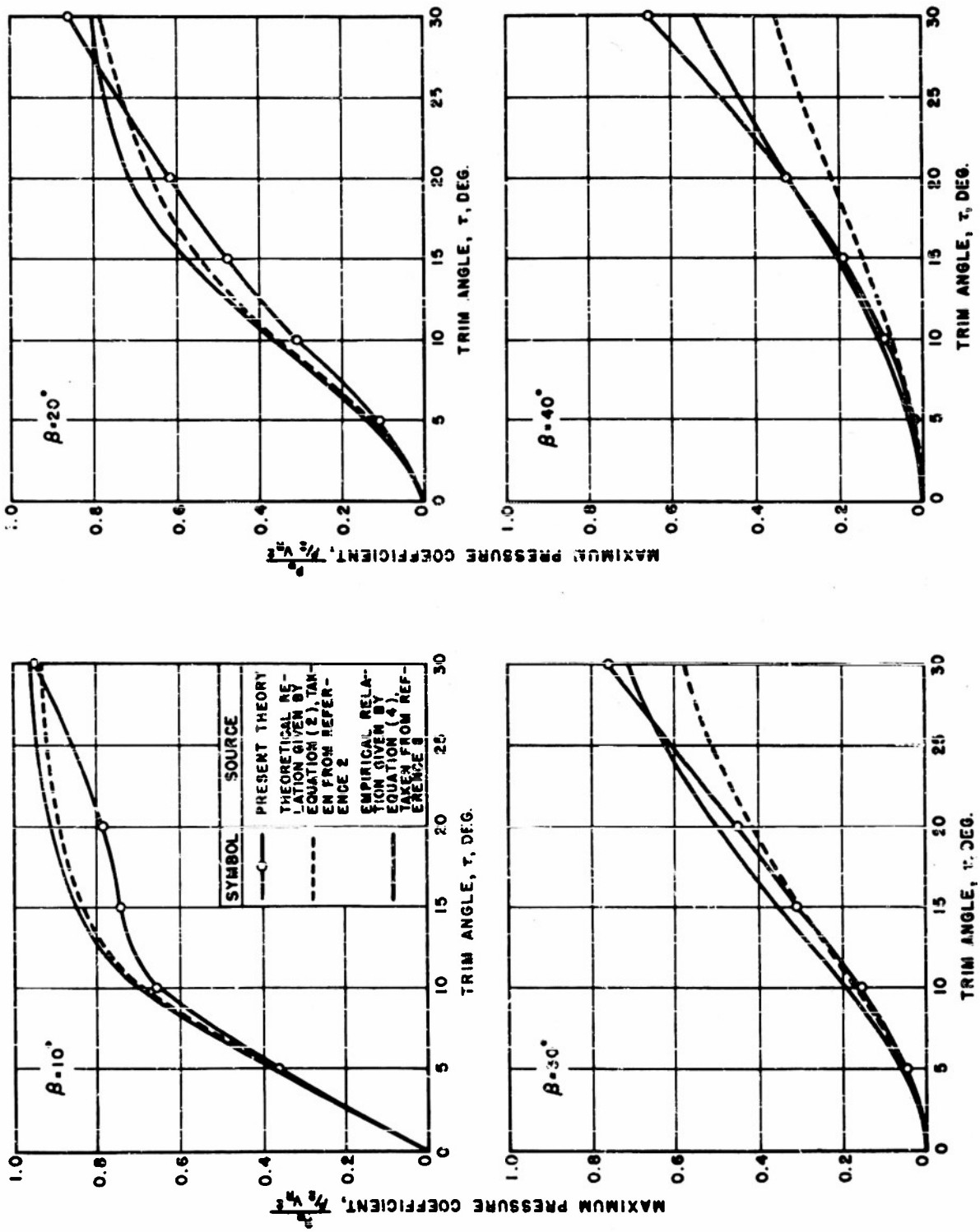

FIGURE 9
VARIATION OF THEORETICAL MAXIMUM PRESSURE COEFFICIENT WITH TRIM ANGLE

FIGURE 10

VARIATION OF EMPIRICAL DEADRISE CONSTANT J
WITH PLANING BODY DEADRISE ANGLE

$$\frac{p_m}{\rho/2\, V_0^2} = \frac{\sin^2 \tau}{\sin^2 \tau + J^2 \cos^2 \tau}$$

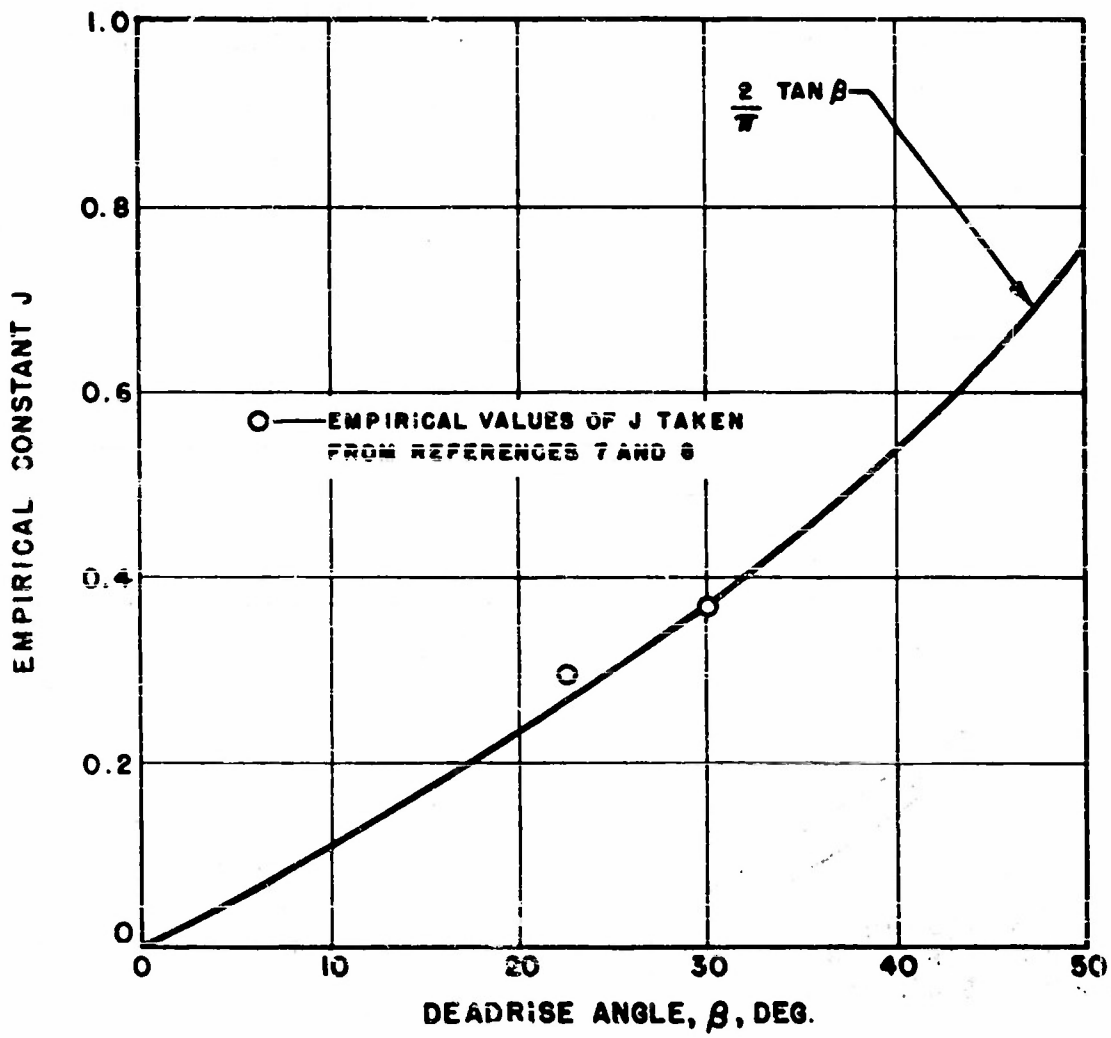

FIGURE 11

A PLAN VIEW OF THE PLANING BODY
WITH SECTIONAL PRESSURE CONTOURS

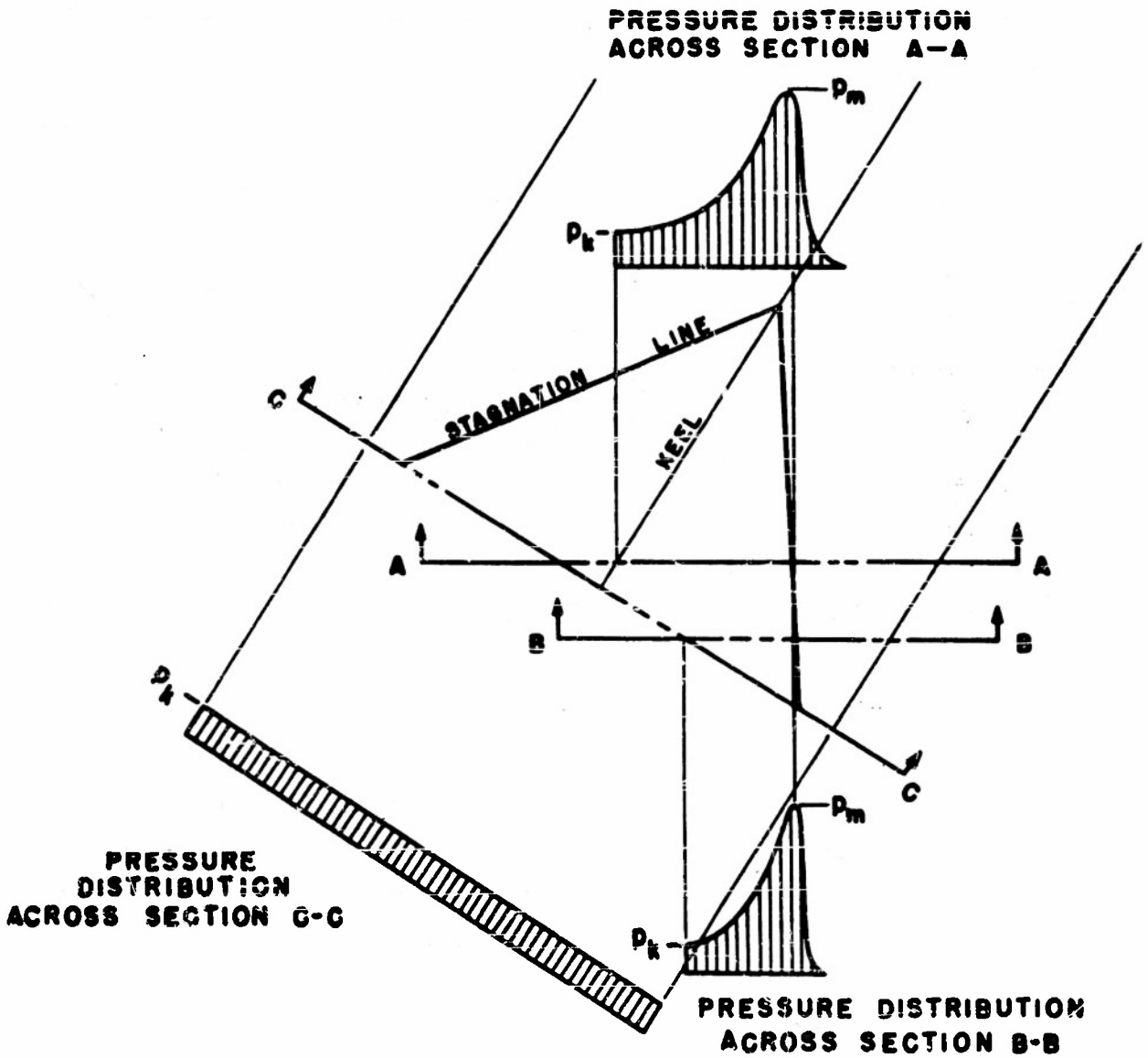

FIGURE 12
PRESSURE DISTRIBUTION
OVER IMMERSING WEDGE
(CURVES REPRODUCED FROM REFERENCE 1)

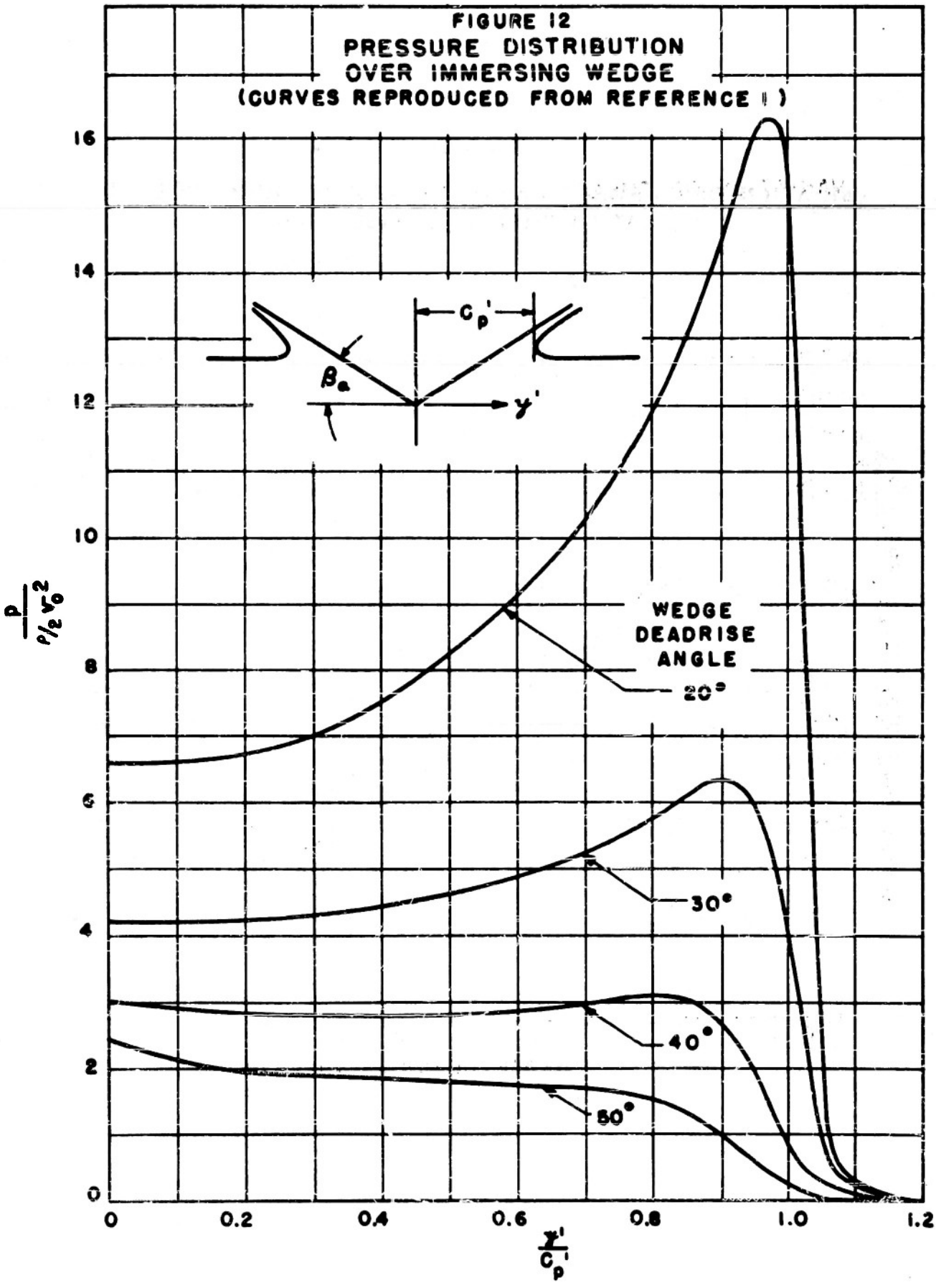

FIGURE 13

VARIATION OF THEORETICAL AVERAGE PRESSURE COEFFICENTS WITH WEDGE DEADRISE ANGLE

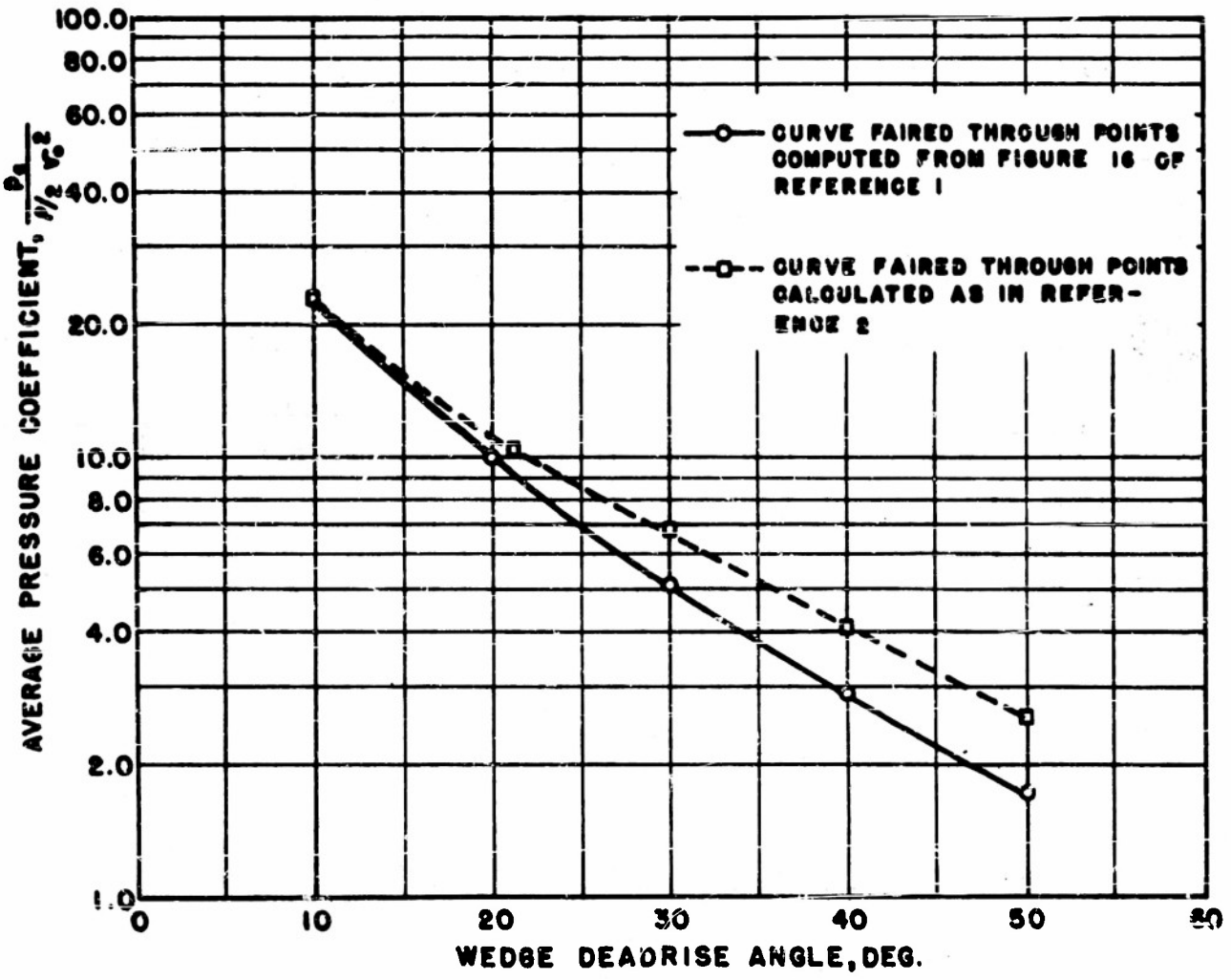

FIGURE 14

COMPARISON OF EXPERIMENTAL AND THEORETICAL DIMENSIONLESS WETTED AREA

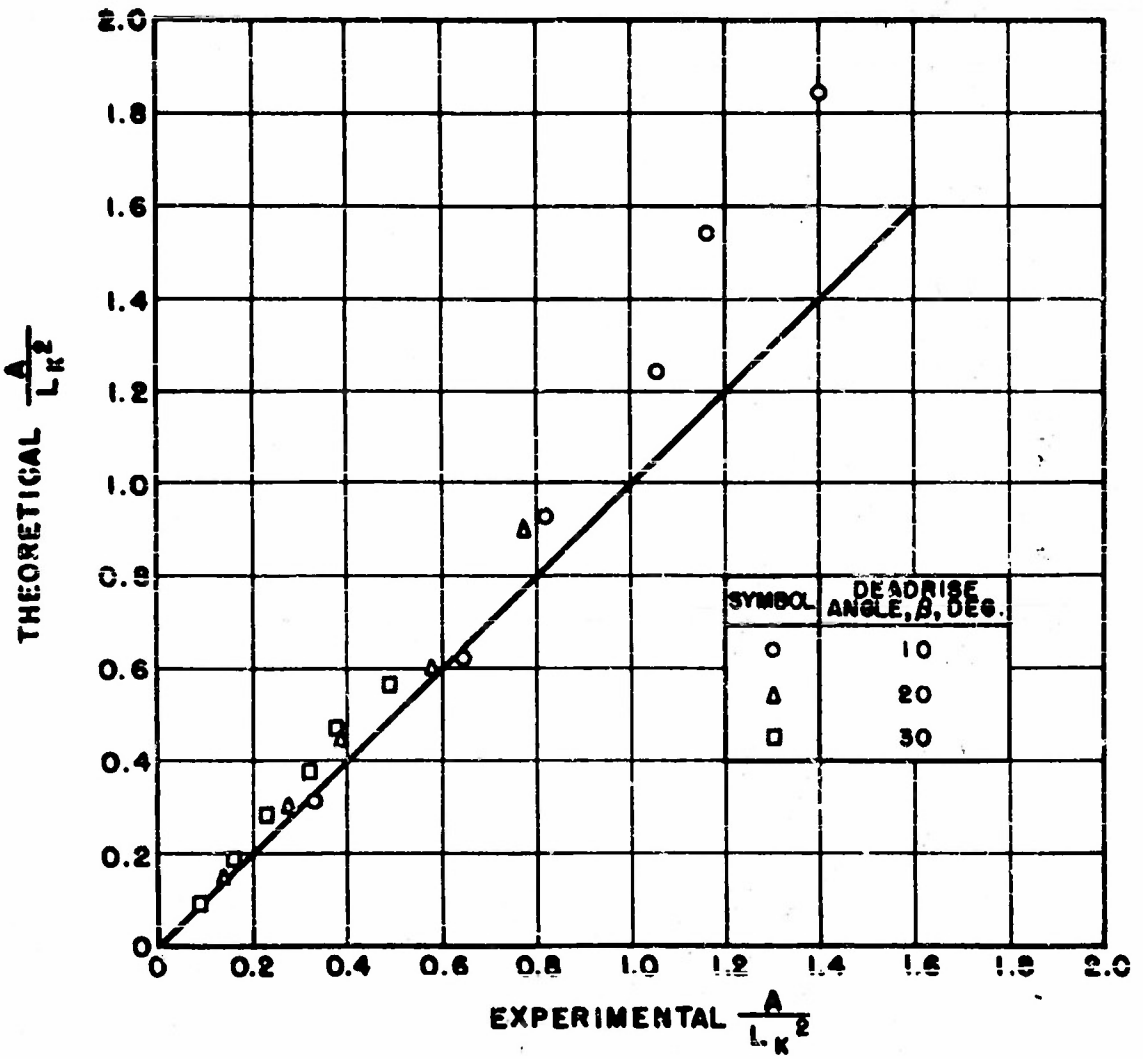

FIGURE 18

VARIATION OF $\frac{\pi}{2}$ SIN τ/TAN β
WITH PLANING BODY DEADRISE AND TRIM ANGLES

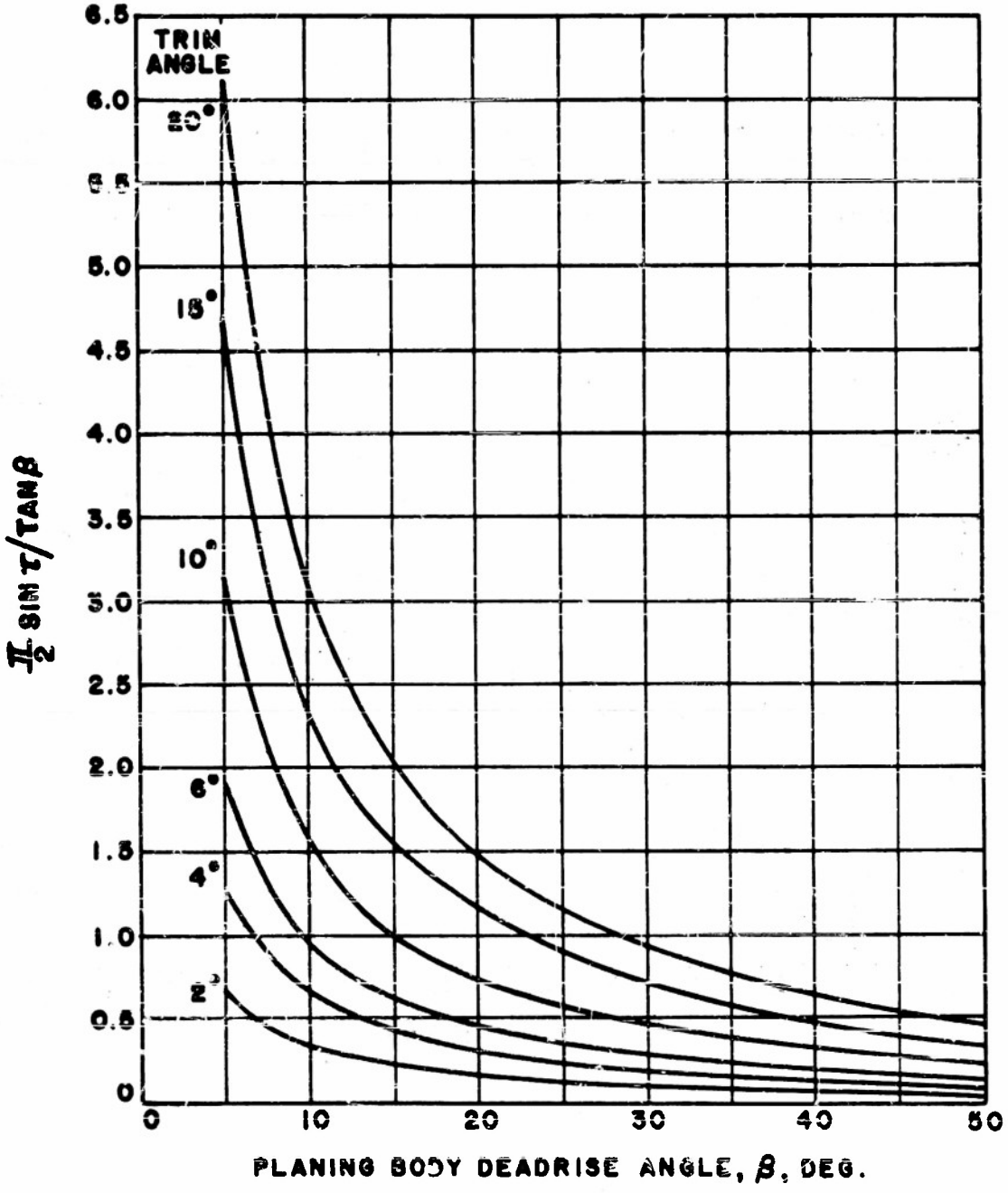

FIGURE 16

VARIATIONS OF THEORETICAL AND EXPERIMENTAL LIFT COEFFICENTS WITH $\lambda' \cos^2 \beta$

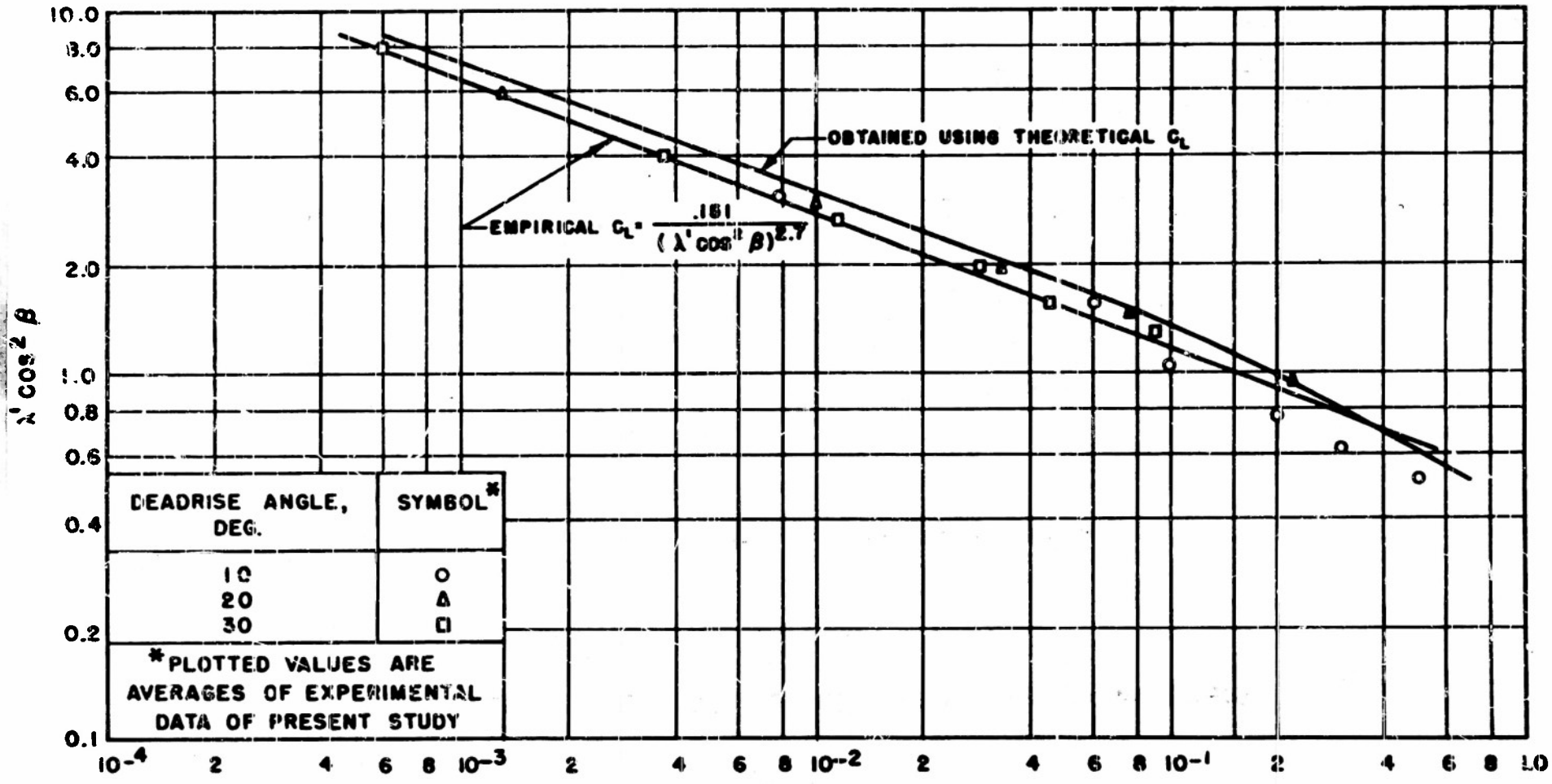

LIFT COEFFICIENT, $C_L = \frac{L}{\rho/2 V_B^2 L_K^2}$

FIGURE 17

THE REFERENCE SYSTEMS FOR THE STABILITY ANALYSIS

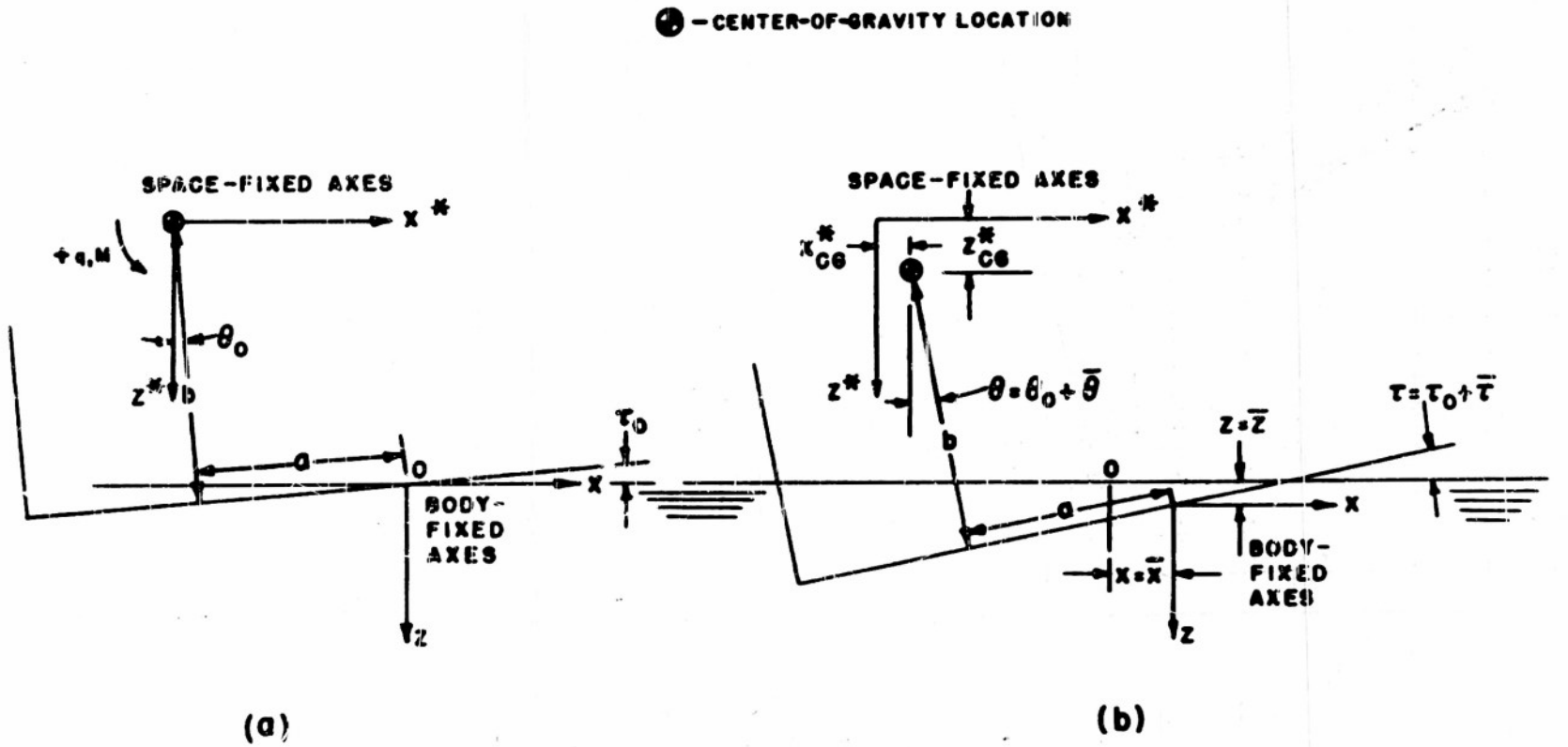

FIGURE 18

TRUE VIEW OF ONE SIDE OF THE SYMMETRICAL WETTED AREA OF THE PLANING BODY

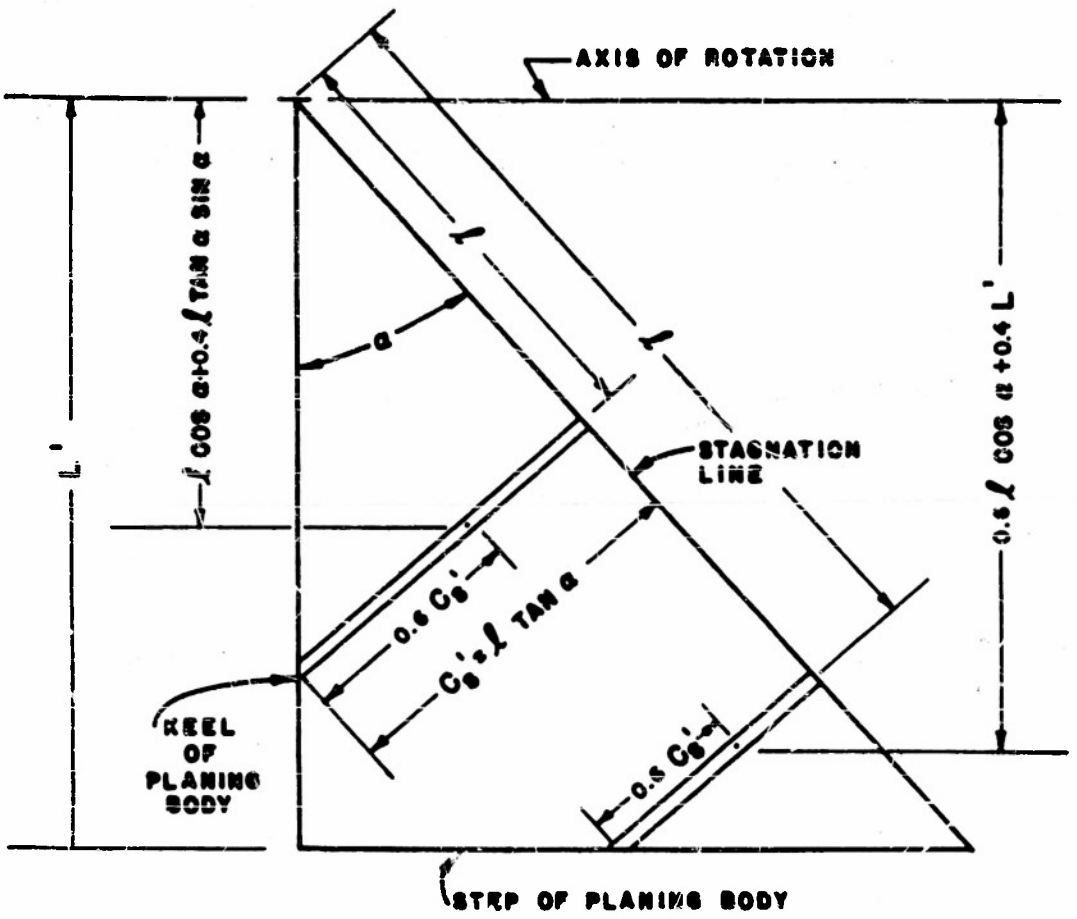

FIGURE 19

VARIATION OF $F_1(\alpha)$ AND $F_2(\alpha)$
WITH THE ANGLE BETWEEN THE KEEL AND STAGNATION LINES

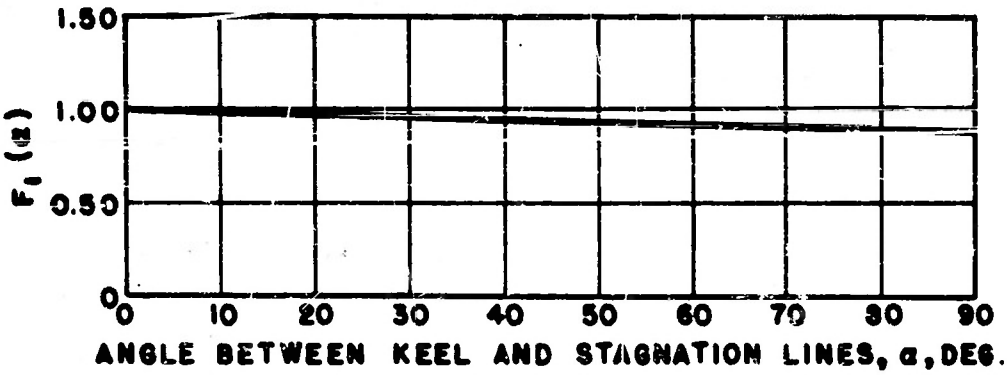

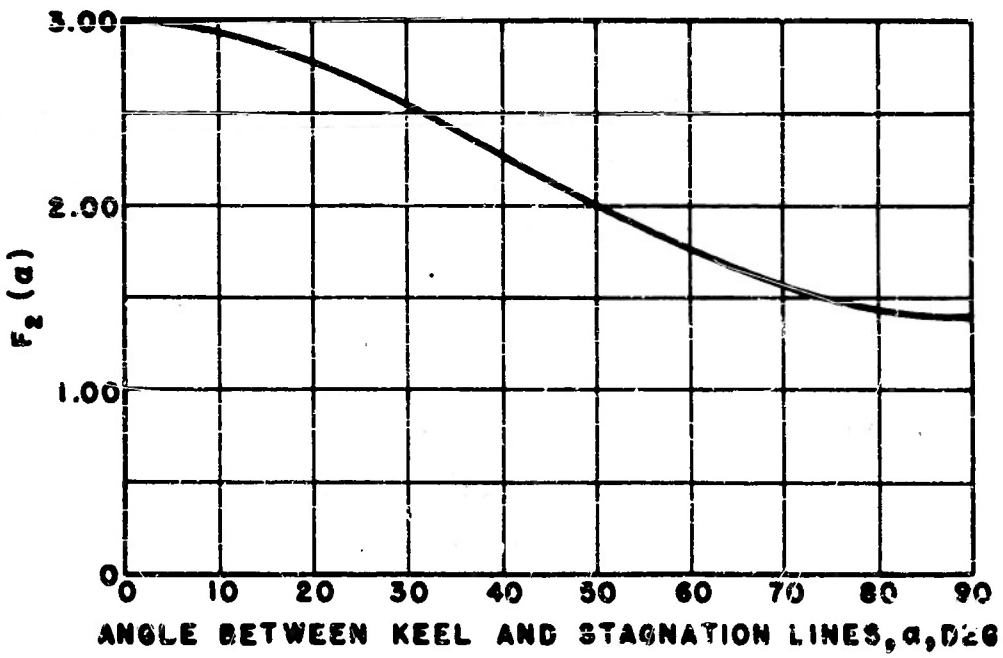

FIGURE B-1

VARIATION OF DEADRISE FACTOR K WITH WEDGE DEADRISE ANGLE

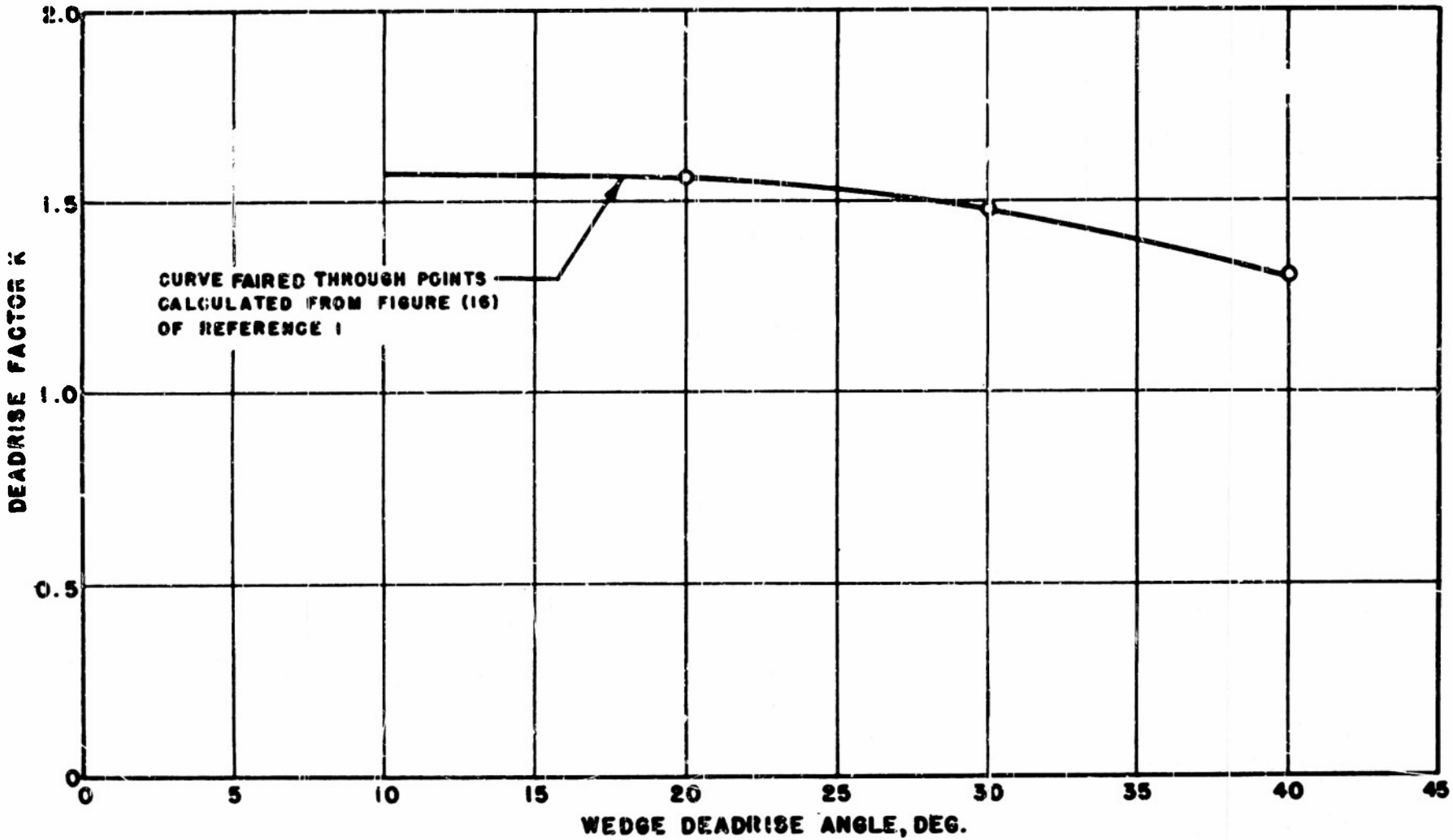

AD 453288

UNCLASSIFIED